The output of both operational amplifiers is +10 volts to -10 volts. Ampere-hours are displayed on a voltmeter whose scale is calibrated from 0 to 100 ampere hours; watt-hours are displayed on a voltmeter whose scale is calibrated from 0 to 2.5 kilowatt hours. At the start of discharge the ampere-hour meter will reset to 70 ampere-hours, and the watt-hour meter will reset to 1.75 kilowatt hours.

CONTRACT NAS 9-6470

DEVELOPMENT AND FABRICATION OF ADVANCED BATTERY ENERGY STORAGE SYSTEM

Prepared by

THE BOEING COMPANY
SPACE DIVISION
SEATTLE, WASHINGTON

Sidney Gross - Technical Leader

April 10, 1967

MID-TERM REPORT

September 27, 1966 through

March 26, 1967

Prepared for

National Aeronautics and Space Administration
Manned Spacecraft Center
Houston, Texas

CONTENTS

1. INTRODUCTION

The Manned Spacecraft Center of NASA has contracted with The Boeing Company for the development and fabrication of an advanced battery energy storage system using vented silver-cadmium cells. The contract number is NAS 9-6470. The work was started on September 27, 1966, and will be completed, except for the final report, on September 27, 1967. This document is a mid-term report, which summarizes the accomplishments during the first six months.

The objective of this program is to develop a silver-cadmium secondary battery energy storage system to meet the power requirements of manned orbital missions of up to one year in duration. Boeing's major tasks are:

1) Develop and provide eight silver-cadmium batteries of more than 70 ampere-hours capacity each, constructed from vented cells.
2) Develop and provide four charge-discharge controllers for cycling the batteries, plus instruction manuals.
3) Perform a detailed thermal analysis of the battery to accurately predict heat generation and temperatures over a wide range of operating modes. A computer program for performing the thermal analysis is to be delivered.
4) Provide calorimeters for measurement of internal heat generation in two specially instrumented batteries.

Important work has been completed in the areas of cell design, venting system, battery packaging, calorimeter design, and the battery charge-discharge controller. Each of these areas is the subject of a chapter in this mid-term report. Each chapter starts with a summary of the pertinent contract requirements, and continues with a discussion of the results obtained during the first six months of the contract period.

2. PROGRAM STATUS

Figure 1 summarizes the program status and shows the major milestones. Progress on all tasks is on schedule. Cells for the battery have been designed and prototype cells are now being tested. The battery package has been designed, and thermal analyses are proceeding based on this design. Typical heat generation experiments have been conducted, and a generalized correlation has been developed. A calorimeter concept has been selected, and detailed calorimeter design trades have started.

Design of the charge-discharge controller has been completed. Components have been selected and ordered, and assembly of the cabinets has been started. Ampere-hour and watt-hour meters with analog output have been developed for monitoring the batteries during test.

No serious problems have appeared.

PROGRAM SCHEDULE

BATTERY DEVELOPMENT, CONTRACT NAS 9-6470

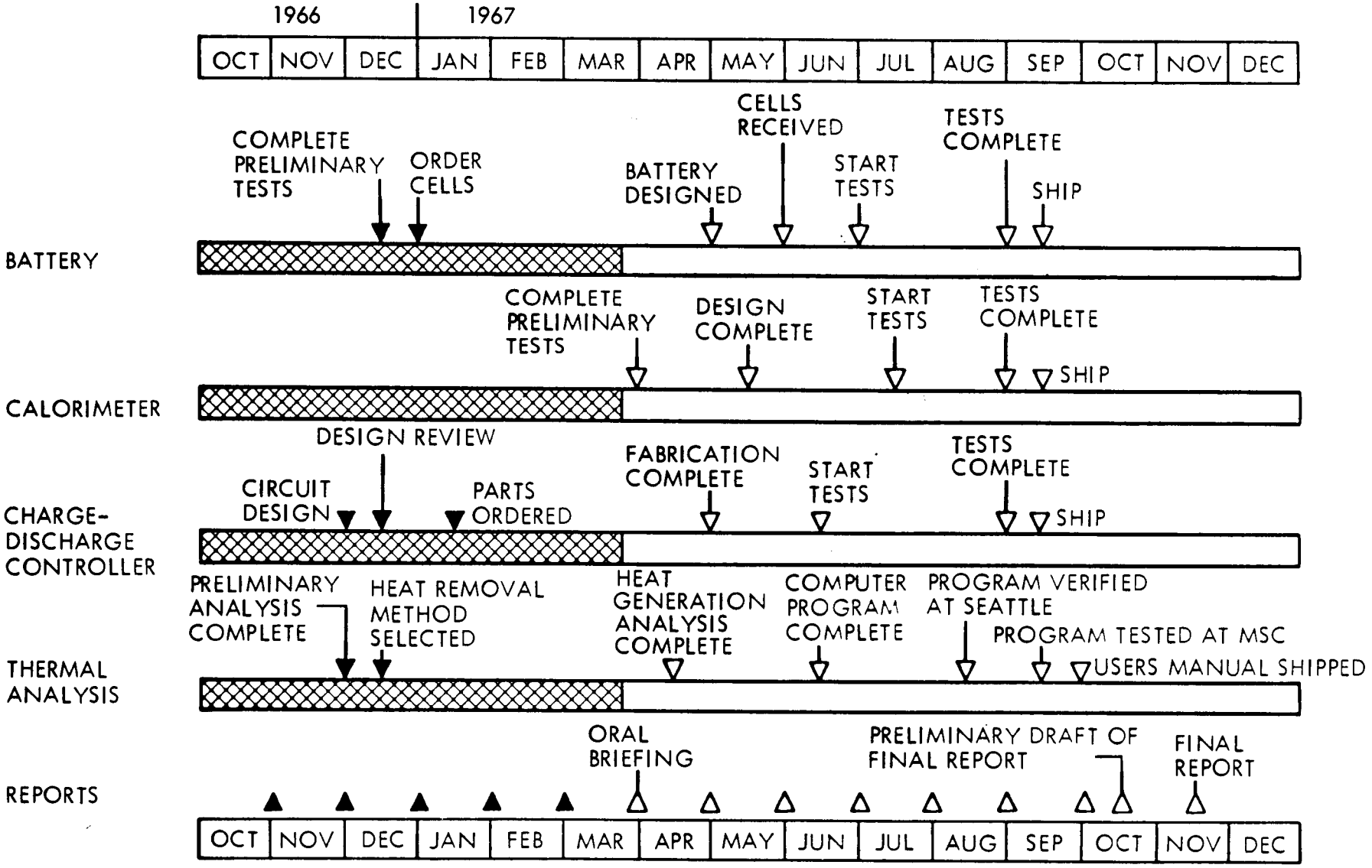

FIGURE 1

3. CELL DESIGN

REQUIREMENTS

The electrical performance requirements of the cells are as follows:

1. Nominal Cell Rating. Cell rating at a C/2 rate of discharge to an end voltage of 0.6 volts shall be greater than 70 ampere-hours with cells operating between 60°F to 90°F. At the end of a 75 percent depth of discharge on this test, battery voltage shall be greater than 28.0 volts.
2. Cycling Capability. When packaged as a battery of 28 series-connected cells, the cells shall be capable of operation under the following range of test conditions with programmed and fixed loads:
   a) At least 5500 charge/discharge cycles at 25 percent depth of discharge with a 58-minute charge, 36-minute discharge cycle.
   b) At least 200 charge/discharge cycles at 75 percent depth of discharge with a ten-hour charge, two-hour discharge.
   c) At least 100 charge/discharge cycles at up to 75 percent depth of discharge on a 24-hour cycle (22-hour charge, two-hour discharge) with a widely varying load which includes peaks having a maximum duration of ten seconds at a 3C rate.
3. Cell Voltage. The battery steady-state voltage shall not fall below 25 volts during the above testing.

Environmental requirements are that the battery operates in the pressure range of 10^{-6} mm Hg to 760 mm Hg, and in an ambient temperature range of 0 to 160°F when mounted on coldplating having a temperature range of 60 to 90°F.

It should be made clear that the objective of this program was to build batteries with vented cells for laboratory testing. Thus, trade studies of vented cells versus sealed cells were not made. Furthermore, the battery is not required to be a flight prototype.

In order to insure meeting the above requirements, The Boeing Company has specified that there be careful quality control during cell manufacture. The weight and density of all plates are controlled. Allowable deviations from average values are as follows:

	Negative Plates (Cadmium)	Positive Plates (Silver)
Deviation from average plate thickness	0.002 inches	0.001 inches
Deviation from average plate weight	4 percent	2 percent

WORK COMPLETED

Yardney Electric Corporation was selected to build the cells. Preliminary design of the cells has been completed, some prototype cells have been built, and the prototype cells are being tested to verify performance. Production of cells will start after electrical performance has been proven by test.

Eight prototype cells have been built for test, and the weight and thickness of all the plates used in these cells have been recorded. Figure 2 summarizes the data for the negative plates, and Figure 3 summarizes the data on the positive plates. These data show that the plate variations are within the required tolerances.

WEIGHT AND THICKNESS VARIATION OF NEGATIVE PLATES

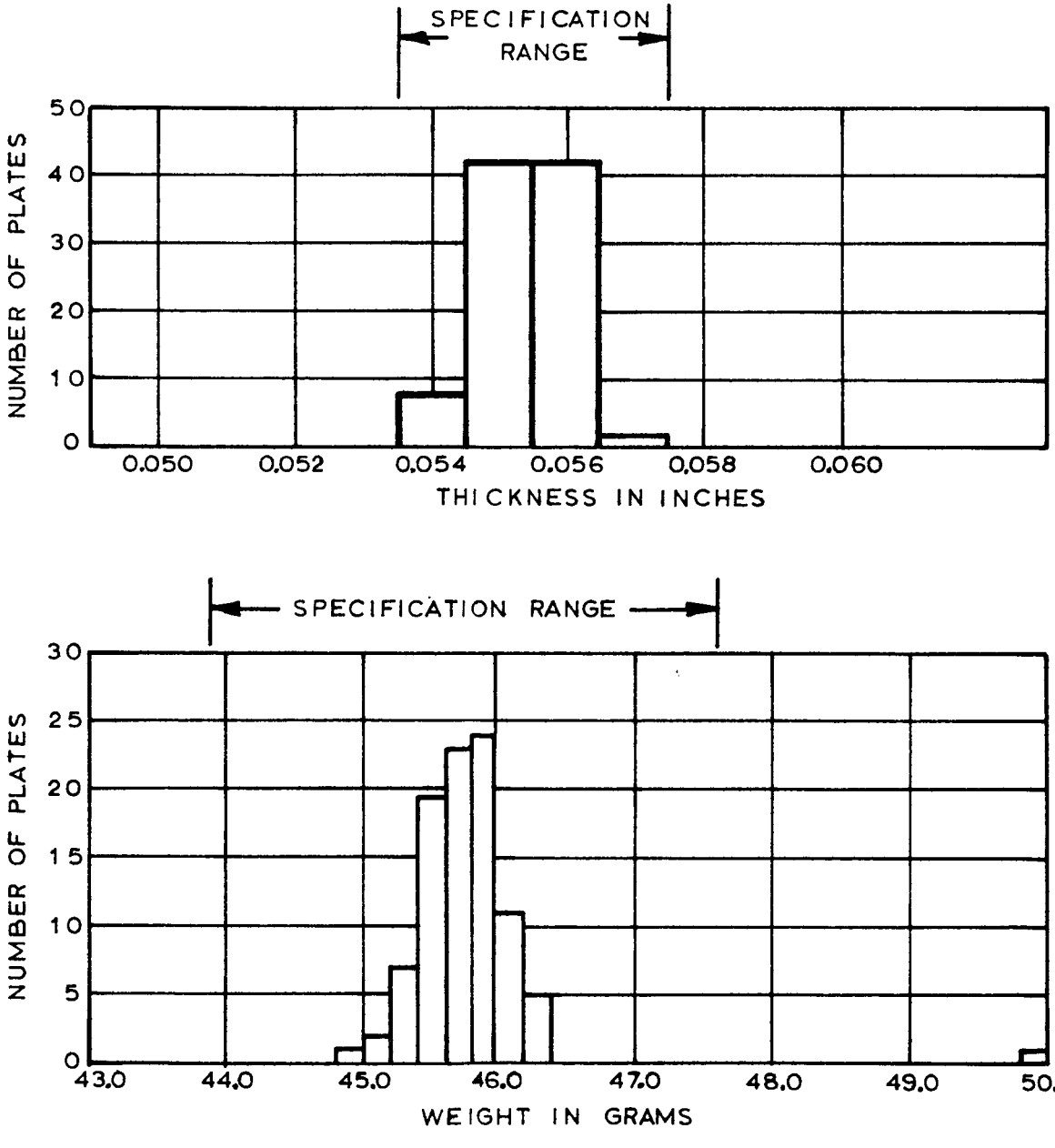

FIGURE 2

WEIGHT AND THICKNESS VARIATION OF POSITIVE PLATES

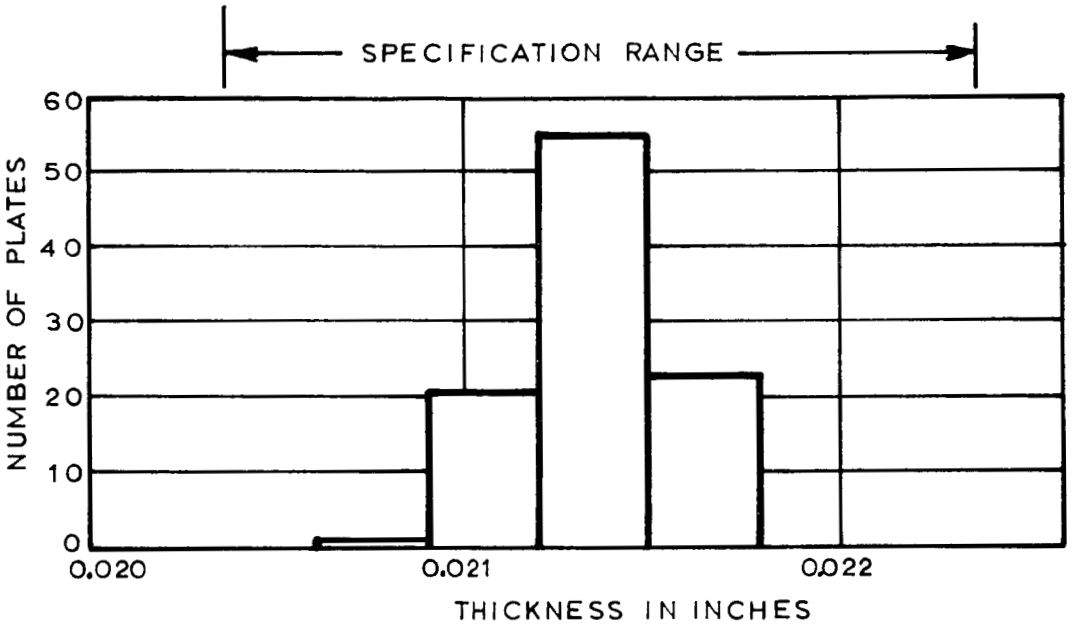

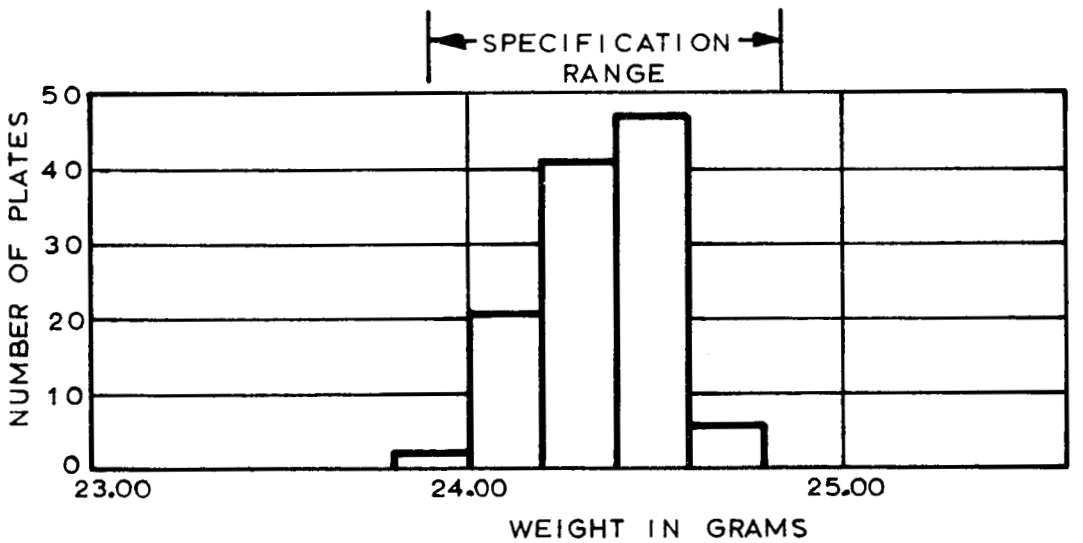

FIGURE 3

The estimated weight of the cell is 3.17 pounds. This will result in a weight of 88.8 pounds for the 28 cells, not including packaging. Thus, the weight of the packaged battery will exceed the design weight goal of 85 pounds.

The cell case will be made from a styrene acrylonitrile copolymer. Though this material is not so good thermally as some other plastics, it was selected because its transparency is important in quality control inspection. The cell will have a Swagelock fitting for attachment of vent lines.

Cell dimensions will be: height, 8.5 inches including terminals; width, 2.81 inches; and depth, 1.75 inches. Each cell will contain 12 positive and 13 negative electrodes, with each electrode 2.32 by 6.19 inches. The positive electrodes will have a total area of 345 square inches to yield a maximum discharge current density (at 210 amps) of 0.61 amperes per square inch. The separators are pellon and modified cellulose (C-19).

The maximum expected pressure in the cells is 4.4 psig. To assure that the cell cases are capable of withstanding this pressure, burst tests were conducted on three empty cell cases. These cases failed at 45, 50, and 55 psig. This test demonstrated that there is sufficient strength margin, and suggests that cell-case thickness and weight could be reduced in a flight battery.

4. VENTING

REQUIREMENTS

Venting of the cells is required to limit gas pressure within cells during charge and during inadvertant cell reversal. The venting system must also maintain a minimum cell pressure during operation at ambient pressures as low as 10^{-6} mm Hg. Pressure-measuring instrumentation is also required.

WORK COMPLETED

As silver cadmium cells approach full charge, part of the current goes into the charge reactions, and some goes into the production of gaseous oxygen. It was necessary to obtain quantitative data on gassing rates to provide criteria for the design of the venting system and also to help determine the best charge control settings.

The test setup used to obtain gassing data is shown in Figure 4. Cells were placed in a water bath having controlled temperature, and the rate of gas evolution was measured by displacement of water in glass tubes. The tubes were adjustable in height to eliminate pressure differentials; a micro-rotometer was used to measure high gas flow rates.

Steady state gassing rates at constant voltage appear in Figure 5. These data show that operation at elevated temperature results in higher gassing rates, and also causes the onset of gassing to occur at lower voltages. Thus, to minimize gas evolution, high temperatures and high charging voltages should be avoided.

Figure 6 shows typical transient gassing rates as the cell approaches full charge. These data show that to minimize gassing the charge should be terminated before the current stabilizes to its lower level.

GAS EVOLUTION RATE MEASUREMENT TEST

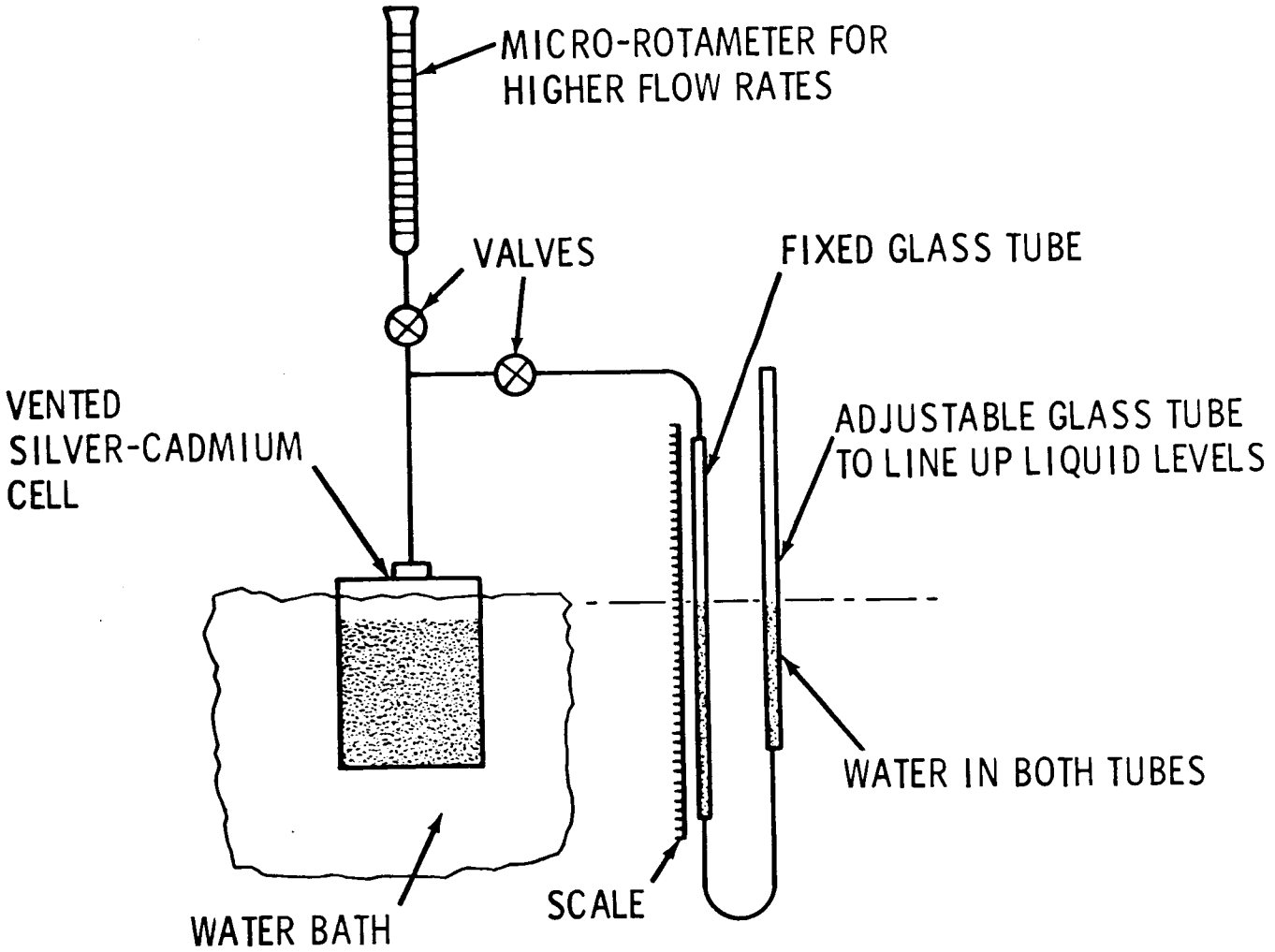

FIGURE 4

GASSING RATES AT CONSTANT POTENTIAL OVERCHARGE

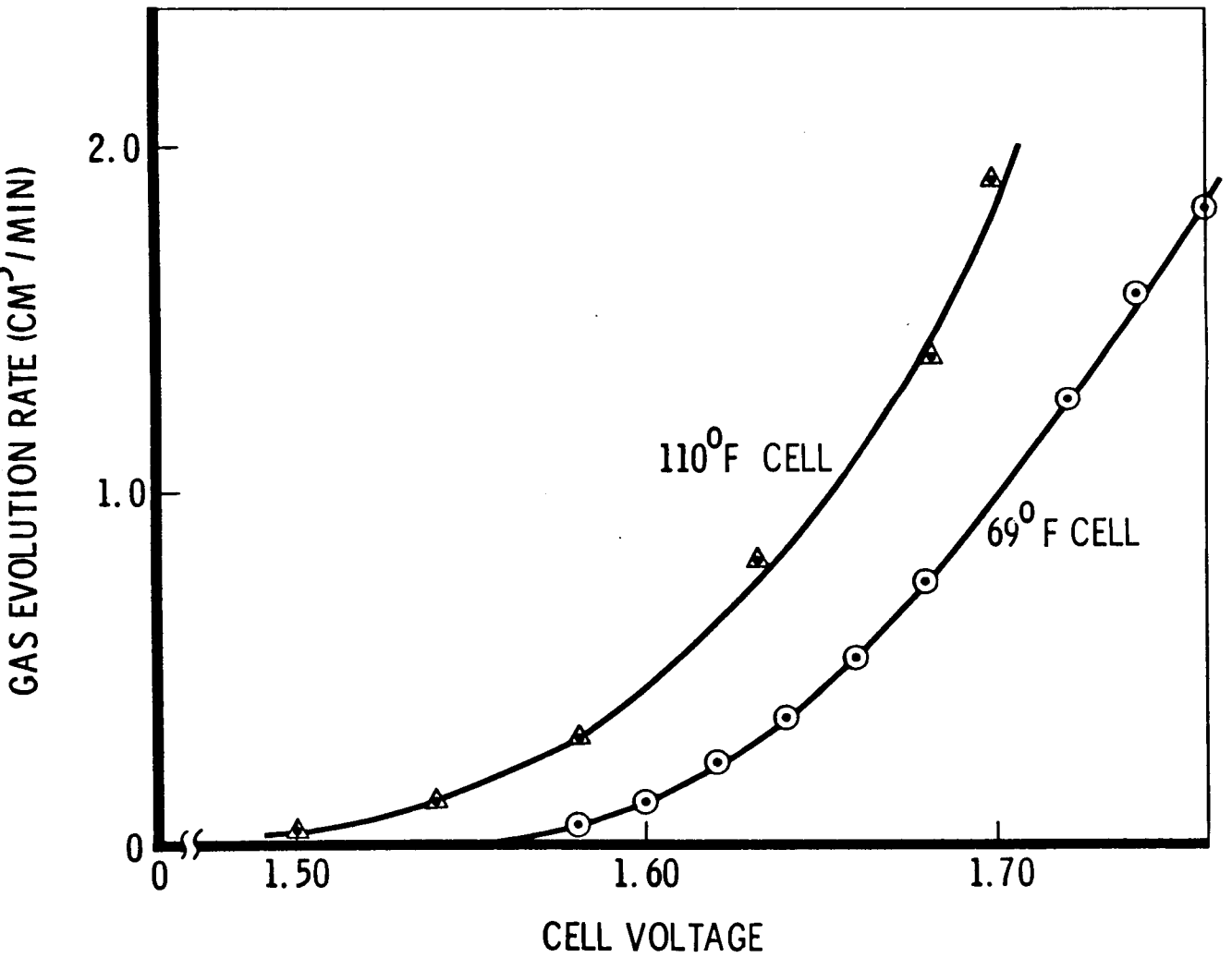

BASIS

CURRENT DECAYED TO NEAR ASYMPTOTE LEVEL

FIGURE 5

TRANSIENT GASSING RATES AT END OF CHARGE

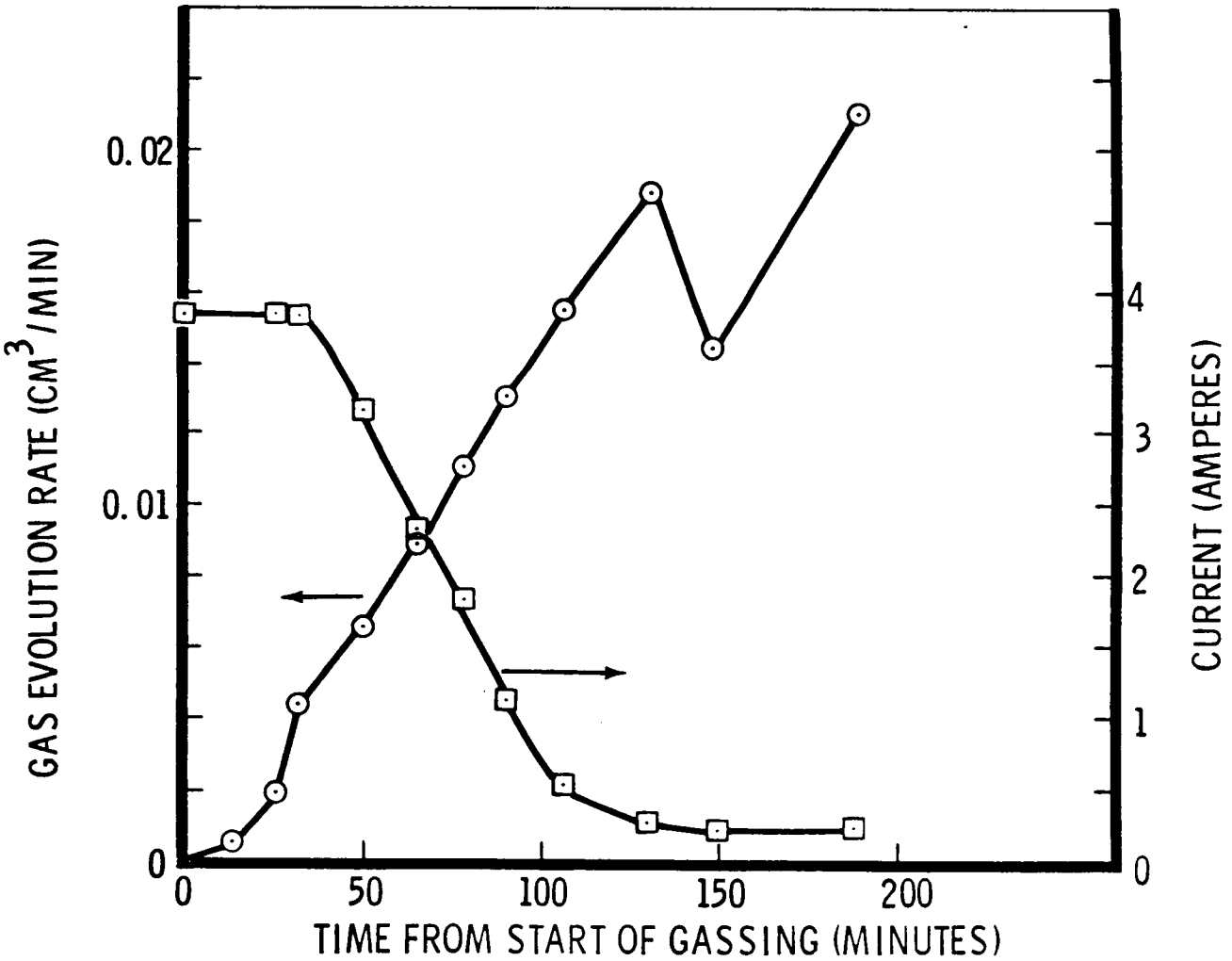

BASIS

- CHARGE AT 3.9 AMPERES TO 1.55 VOLTS
- CELL TEMPERATURE = 70°F

FIGURE 6

Operation of the battery at low pressures is expected to cause gassing to start at lower voltages. The magnitude of this effect was calculated. Assuming 3.5 psia in the cell, the calculation showed that gassing will start at 0.01 volts less than at atmospheric pressure.

A sample was collected of the gas evolved at the maximum voltage used in the gassing tests (2.12 volts). The gas was analyzed in a high resolution mass spectrometer, and the results are shown in Table 1. As expected, the gas was mostly oxygen, and the remaining gases detected were in very minute quantities. It is concluded, therefore, that venting of a silver cadmium battery to the interior of a spacecraft should not cause a health hazard. No hydrogen was present, and it is assumed that hydrogen will not be evolved at lower voltages, at least until the cadmium electrode reaches a high state of charge (which requires considerable prior gassing).

The cell venting system planned is shown in Figure 7. All 28 cells are connected to a common manifold having a single pressure relief valve. A removable CO_2 scrubber is provided to prevent carbonate formation at the relief valve during storage, and a filter is provided to minimize inadvertant contamination of the relief valve and the pressure transducer.

Two items in the vent system were considered to be critical. One was the separation of gas and vapor in each cell, to prevent liquid carryover into the manifolding. The other was the reliability and performance of the pressure relief valve. Tests conducted on these two items have resulted in satisfactory solutions. Results of these investigations are summarized below:

Liquid Vapor Separation. Flight qualified vented batteries will require a means to separate liquid and gas during venting. Though beyond the scope of this program, an attempt was made to see if a simple device could be incorporated into the vent port design to achieve separation at

Table 1

SPECTROSCOPIC ANALYSIS OF EVOLVED
GAS DURING OVERCHARGE

Molecular Weight	Gas	Approximate Quantity	Comment
15	CH_4	Slight Trace	*
18	H_2O	Nearly Saturated	Expected
20	Ne	Very Slight Trace	Atmospheric Tract
28	N_2	Less than 1%	Diluent Gas
29	C_2H_4	Slight Trace	*
32	O_2	Almost 100%	Expected
33	$O^{16}=O^{17}$	Very Slight Trace	Natural Isotope
34	$O^{16}=O^{18}$	Trace	Natural Isotope
40	A	Slight Trace	Atmospheric Trace
41	Hydrocarbon	Very Slight Trace	*
43	Hydrocarbon	Very Slight Trace	*
44	CO_2	Trace	

* Possibly from Apezone grease or Tygon tubing

CELL VENTING SYSTEM

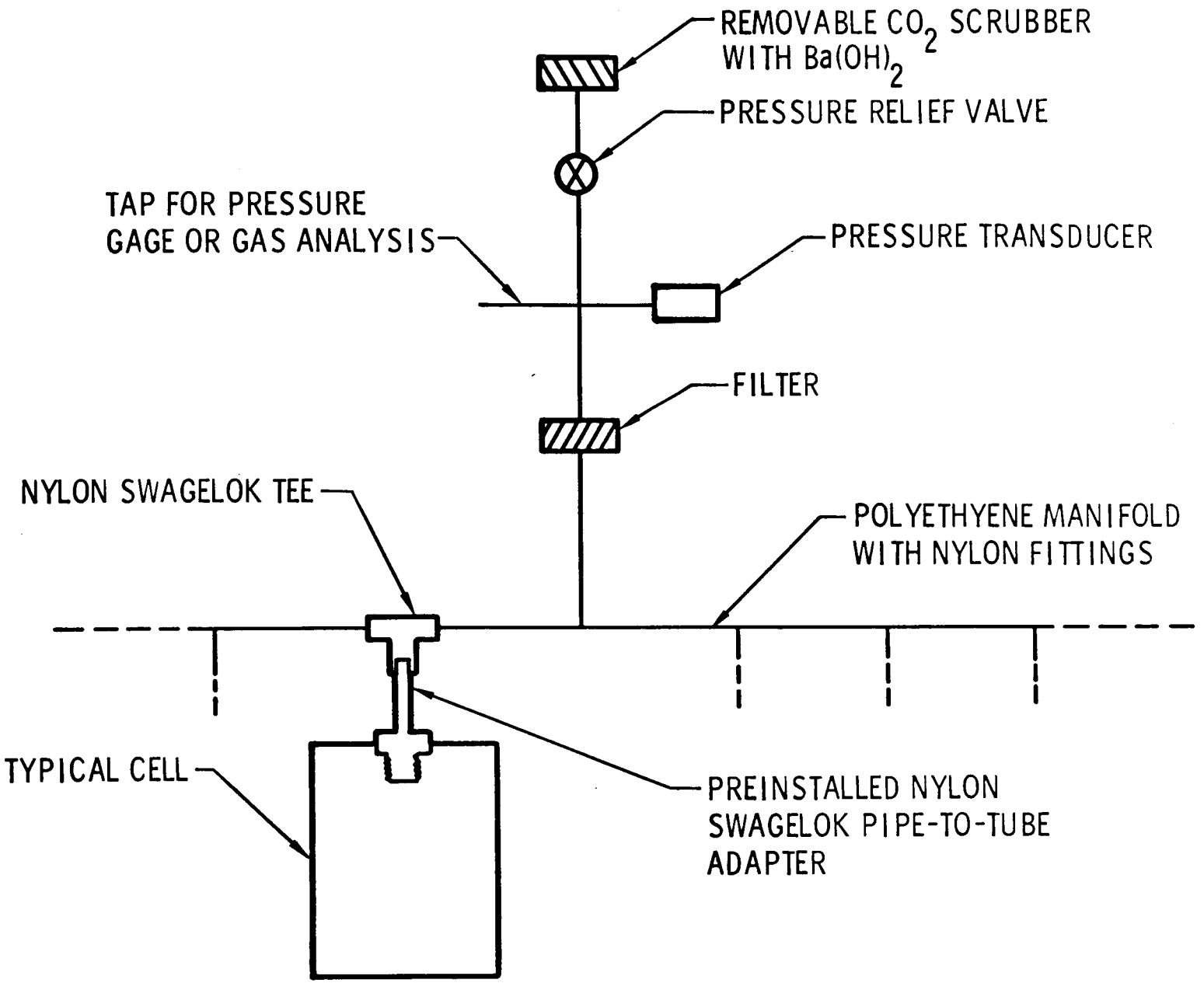

FIGURE 7

very low gravity. Theoretical studies show the possibility of designing a phase-separating vent based on the low wettability of teflon. Various teflon and other materials were therefore acquired and tested for effectiveness as a phase separator. The following conclusions result from the vapor-liquid separation studies and tests:

1. Liquid carryover by gas during venting under gravity conditions is not expected to be a problem since carryover occurs at vent rates approximately six times higher than the maximum vent rates contemplated.
2. Some type of separation device should be used to trap fine mist, and to confine the electrolyte during occasional sloshing or splashing.
3. Teflon repells KOH solution well enough to show promise as a liquid-gas separation mechanism for very low gravity.

Based on these studies, phase separation for the cells for this program will be achieved by sufficient spacing of the vent above the liquid, and by the use of teflon felt in the vent to trap fine mist.

Pressure Relief Valve. A quest for a good pressure relief valve resulted in the choice of a James Pond and Clark "Circle-Seal" pressure relief valve. This valve had been used on several prior space programs and showed good promise for this application. The first test conducted on this valve was to determine its leakage characteristics. Figure 8 shows the test set-up used. Air is scrubbed of CO_2, then bubbled through a KOH solution to simulate mist picked up during gassing.

In one test, the sensitivity of the valve to carbonate formation was determined. The valve was subjected to repeated opening and closing, and no CO_2 scrubber was used. Reaction of atmospheric carbon dioxide with potassium hydroxide caused potassium carbonate to form within the valve. The initial effect was increased leakage. As potassium carbonate

PRESSURE RELIEF VALVE LEAKAGE TEST

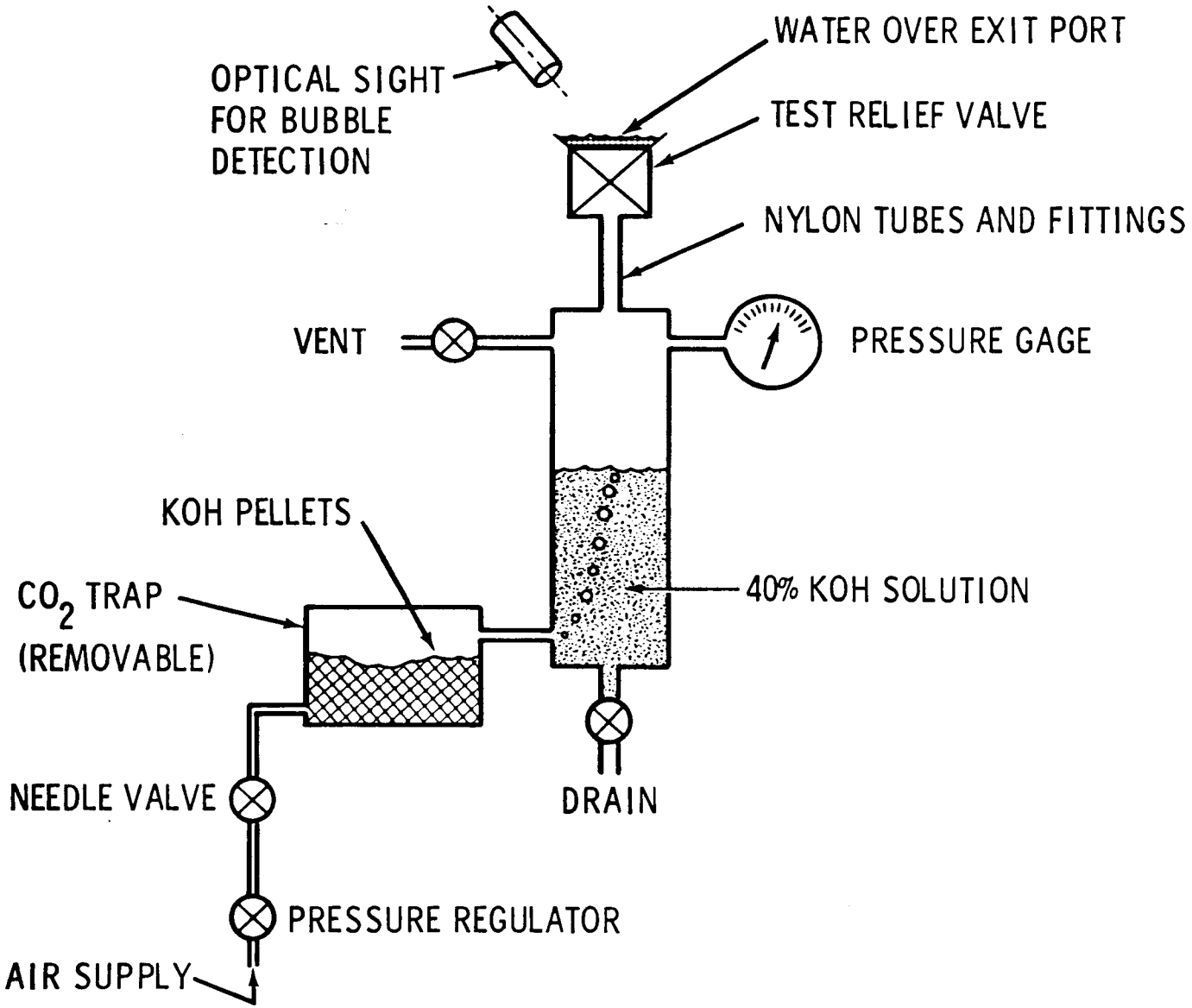

FIGURE 8

built up, however, the valve would occasionally stick shut; once the opening pressure increased from 4.2 psig to 8.1 psig. From this test it was concluded that the valve should be protected from carbonate formation; therefore, a removable cannister containing $Ba(OH)_2$ will be used for CO_2 removal.

In a second test we measured the leakage of a new valve in a simulated life test. KOH corrosion was accelerated by prior immersion of the valve in a KOH solution at 130°F. After ten days, the valve housing was mildly etched, and the grease in the "O" ring seat had disappeared. The "O" ring itself did not appear to be affected, however. This valve was then tested for leakage in the test setup shown in Figure 8, with the CO_2 scrubber installed. Consistent leakage did not appear until approximately three psig was reached, although occasional leakage was observed at lower pressures. Figure 9 shows the highest leakage rates measured.

A reasonable annual oxygen loss in one cell is 1860 cc of gas per year, which corresponds to the electrolysis of 3 cc of water. If one valve is used per cell, the maximum expected leakage is significantly less than 1860 cc per year, as shown in Figure 9. Since one valve will be used to vent 28 cells, the design margin is so large that leakage should not be a problem.

A third concern with the pressure relief valve was whether it would pass gas easily enough to prevent significant pressure rise in the cell. Flow characteristics were therefore tested, and the results are shown in Figure 10. Using gas evolution test data as a basis, an estimate was made of the maximum gassing rate that could occur, also shown in Figure 10. From this study, it was concluded that the maximum pressure in the cell would not exceed 4.4 psig.

MAXIMUM DETECTED LEAKAGE RATE OF PRESSURE RELIEF VALVE

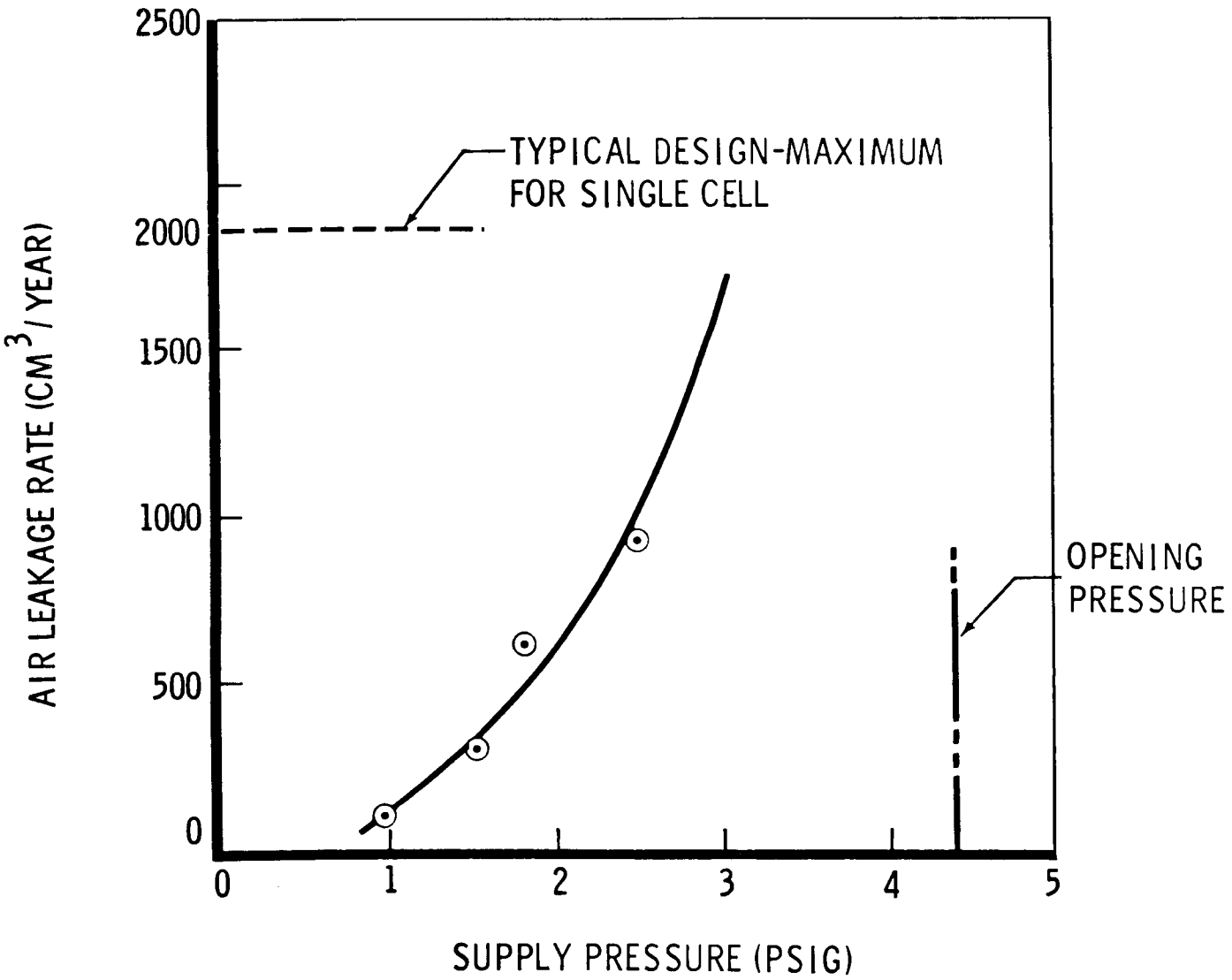

FIGURE 9

FLOW CHARACTERISTICS OF PRESSURE RELIEF VALVE

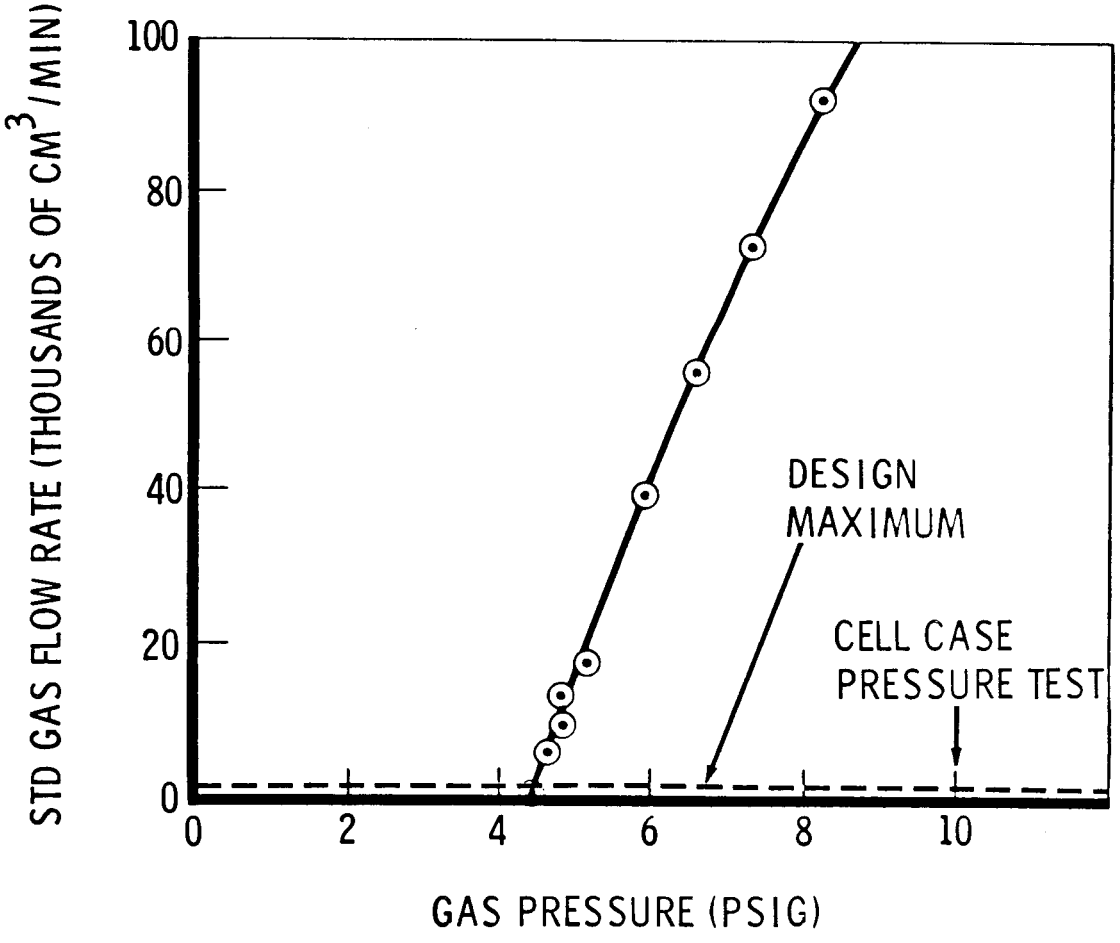

FIGURE 10

5. BATTERY PACKAGING

REQUIREMENTS

The batteries built on this contract are for laboratory use, and are not to be flight prototypes. To meet the requirement of 28 volts minimum, we have chosen to use 28 cells, each of which will provide slightly over one volt per cell. Temperature control of the battery is to be provided by attachment to a NASA-furnished cold plate which will be maintained within the range of 60°F to 90°F. The package must provide for venting of the cells, and must also include instrumentation to measure temperature, pressure and voltage of the cells.

Thermal considerations were emphasized in the packaging of the battery. The thermal design objectives for packaging are:

1. Limit battery temperature. Since the cold plate can be as hot as 90°F, it would be possible for a poorly designed battery to operate at relatively high temperatures. High temperatures result in shortening of life.
2. Obtain uniform cell-to-cell temperatures. Some battery package designs will permit centrally located cells to become hotter than peripheral cells. The objective of balanced cells can be met only if all the cells are at nearly the same temperature.
3. Obtain uniform temperatures within cells. It is desirable that all the plates in a cell come to full charge at the same time, that the current density be uniform, and that material migration be minimum. These objectives will be enhanced if temperature gradients within cells are minimum.

WORK COMPLETED

Thermal Design

A detailed thermal analysis of a single cell was made to determine the best method of removing internally generated heat. This analysis was based on a 3-dimensional heat transfer model of a rectangular cell with

exterior dimensions of 1.75 in. by 2.81 in. by 7.25 in., excluding terminals, which are on the smallest surface and on the top. A cell is composed of 25 plates in a styrene case. Each plate was thermally represented by 20 nodes, resulting in a 530-node model for the cell. Thermal conductances were calculated.

Six conditions were analyzed to determine the basic limitations on temperature control imposed by characteristics of the cell itself:

1. One face isothermal (2.81" x 7.25" surface)
2. One edge isothermal (1.75" x 7.25" surface)
3. Bottom isothermal
4. Terminals isothermal
5. One face and bottom isothermal
6. One face, one edge and bottom isothermal

The isothermal surfaces were heat sinks, held at 70°F. Figure 11 gives the resulting temperature profiles across the centers of the two faces. Results show that the best single surface for heat removal is the face, followed by the edge, bottom, and terminals, in that order. Therefore, further heat removal studies and packaging concepts were based on the use of exterior surfaces, rather than on the use of the terminals.

One possible heat-removal concept uses the cell bottom surface and fins on the two faces. Results of an analysis of this approach are given in Figure 12 for 0.040 in. and 0.080 in. fins. The temperature gradients are small for both fin thicknesses. Further calculations have shown that diminishing returns are obtained from fins thicker than 0.040 in. For example, going from 0.040 in. to 0.080 in. fin thickness reduces the average temperature rise by only 5°F from 22°F.

Using the single cell thermal analyses as a basis, thermal performance guidelines were established to aid in selecting the final packaging design. These guidelines are shown in Table 2.

TEMPERATURE PROFILES FOR Ag-Cd CELL WITH ISOTHERMAL BOUNDARIES

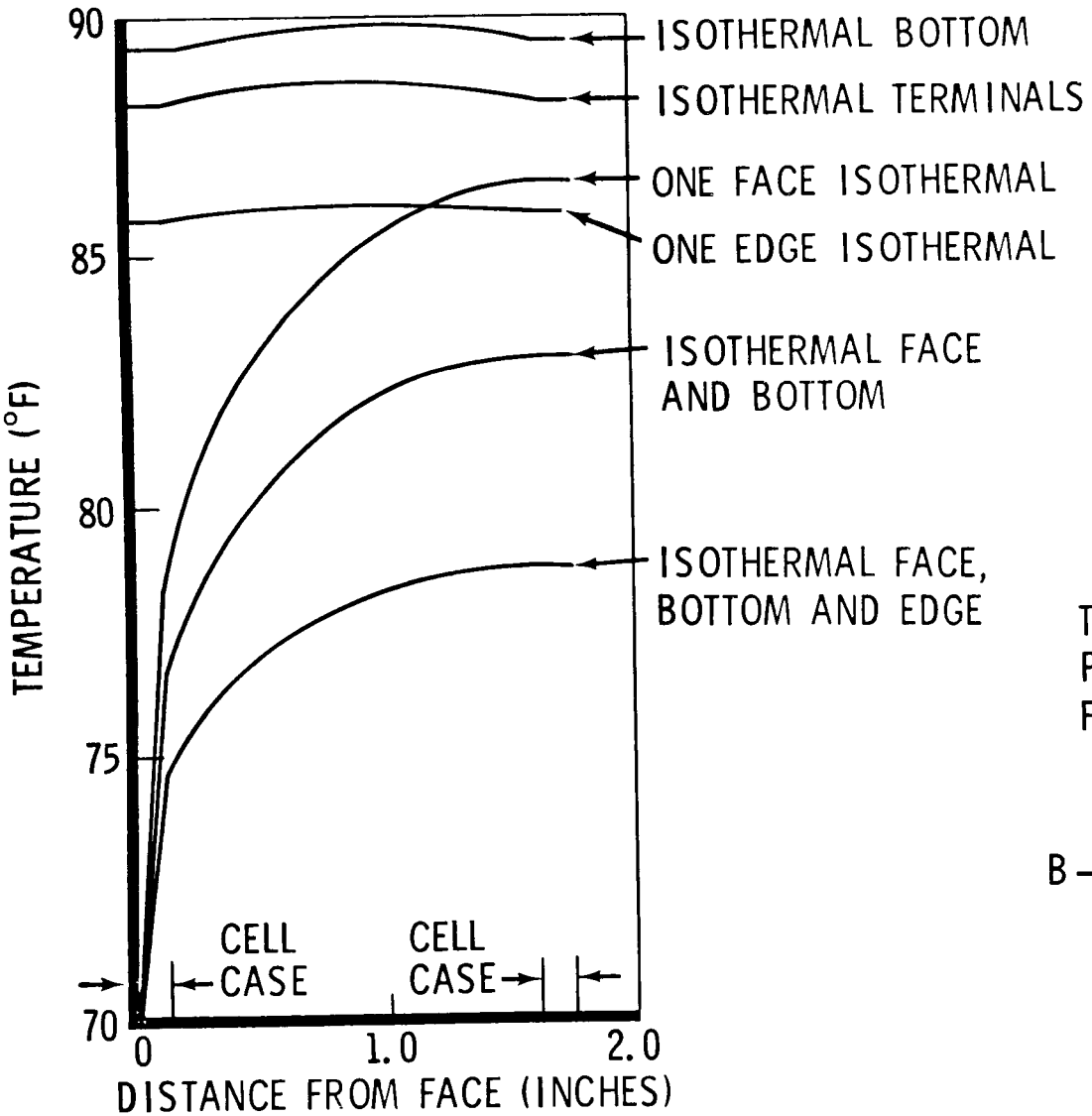

TEMPERATURE PROFILES FROM A TO B

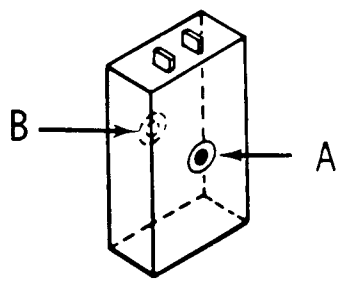

FIGURE 11

Ag-Cd CELL PLATE TEMPERATURES WITH FINS ON TWO FACES AND BOTTOM

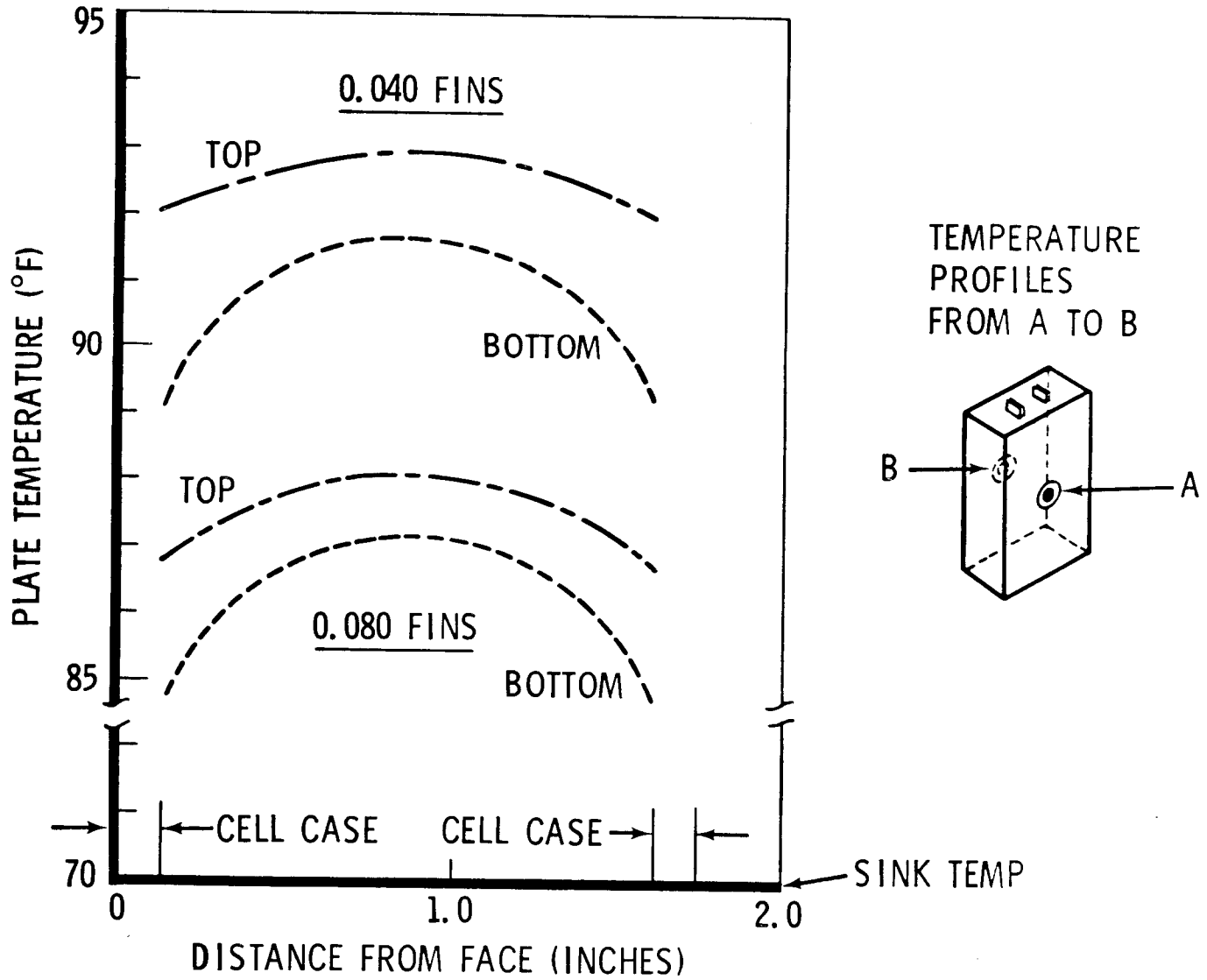

FIGURE 12

TABLE 2

GUIDELINES FOR BATTERY CELL THERMAL CONTROL

CELL COOLING APPROACH		THERMAL PERFORMANCE
One Surface	Terminals Bottom Edge Face	Poor, unacceptable
Two Surfaces	Edge and bottom Face and bottom Face and edge Two edges Two faces	Fair, acceptable
Three Surfaces	Two edges and bottom One face, one edge and bottom Two edges, one face Two faces and bottom Two faces, one edge	
Four Surfaces	Two edges, one face and bottom Two faces, one edge and bottom Two edges, two faces	Good, acceptable
Five Surfaces	Two edges, two faces and bottom	

Material Selection

The major functions of the package material are to conduct heat and provide mechanical support with low weight. The spectrum of possible materials was narrowed to the magnesium and aluminum alloys in Table 3, which also shows their thermal characteristics. Constant weight is believed to the most applicable of the two comparison criteria, and on this basis the magnesium alloys are generally best, although there is a wide spread between the best and the worst magnesium alloys.

Magnesium was selected for packaging. Advantages of magnesium over aluminum for the battery case and heat transport fins are:

1. Higher strength-to-weight ratio.
2. Higher thermal conduction per unit weight.
3. Greater resistance to potassium hydroxide (KOH) attack.
4. Closer match in thermal expansion with cell case.

The disadvantages of magnesium are:

1. Corrodes easily, and the required corrosion protection may increase the thermal resistance between cells and the cold plate.
2. Fabrication is sometimes difficult and costly.
3. Long lead time is needed in acquiring some sizes and alloys.

Initial inquiries on the delivery time of magnesium alloys showed that long lead times might be involved for anything other than thin sheets. Therefore, methods of protecting aluminum from KOH were evaluated to determine if aluminum could be a suitable backup. Tests with a two-step protective coating (BAC 10-16B) showed that good resistance to KOH is achieved if scratches and nicks are absent. This suggests that aluminum could be used if necessary, since KOH would reach the aluminum only in the event of simultaneous cell-case failure, adhesive parting, and damage of the protective coating.

Table 3

THERMAL COMPARISON OF MAGNESIUM AND ALUMINUM ALLOYS

Material		Density (ρ) lb/in^3	Constant Thickness Comparison		Constant Weight Comparison	
			Thermal Conductivity (K) BTU/sec,in,°F	Relative Standing	K/ρ	Relative Standing
Magnesium Alloys	AZ 31B	0.064	1039×10^{-6}	10	1.62×10^{-2}	12
	HM 21A-T5	0.064	1828×10^{-6}	2	2.86×10^{-2}	1
	HK 31A-H24	0.065	1520×10^{-6}	8	2.34×10^{-2}	5
	M1A	0.065	1740×10^{-6}	3	2.68×10^{-2}	2
	ZK60-T6	0.066	1630×10^{-6}	5	2.47×10^{-2}	3
	ZK60A-T5	0.066	1575×10^{-6}	7	2.39×10^{-2}	4
	ZE10A	0.066	1470×10^{-6}	9	2.23×10^{-2}	7
Aluminum Alloys	2014-T6	0.101	1620×10^{-6}	6	2.05×10^{-2}	8
	2024-T3	0.101	1620×10^{-6}	6	1.60×10^{-2}	13
	2024-T4	0.101	1620×10^{-6}	6	1.60×10^{-2}	13
	2219-T6	0.102	1740×10^{-6}	3	1.71×10^{-2}	9
	6061-T6	0.098	2240×10^{-6}	1	2.28×10^{-2}	6
	7075-T6	0.101	1680×10^{-6}	4	1.66×10^{-2}	11
	7079-T6	0.099	1680×10^{-6}	4	1.70×10^{-2}	10

More recent inquiries, however, have produced assurance that we will be able to obtain magnesium of adequate thickness, though not necessarily in the preferred alloys.

The use of an adhesive is planned for thermal and mechanical joining of the cells to the metal case. Properties desired of this adhesive are high thermal conductivity, good adhesion to styrene, high peal strength, good flexibility, and good resistance to KOH. Tests on candidate adhesives showed that a silicon rubber based material (BAC 5010 type 60) will be suitable.

Battery Package Design

After packaging materials studies were made and the thermal design guideline established, 23 packaging design approaches were conceived, studied and evaluated. These concepts differed in geometrical layout, structural arrangement, manufacturing technique, and thermal effectiveness. Table 4 summarizes the designs considered.

In evaluating these concepts, substantial weight was given to thermal considerations. Table 5 summarizes the evaluation of battery packaging concepts. This evaluation showed concept 6b to be the best choice, and so a detailed design was made based on this concept. A mockup of the package was constructed (Figure 13). This mockup does not reflect final dimensions of the package, but does show the general arrangement. Some design features are:

1. Cells are laid out in a row two cells wide and 14 cells long.
2. Metal fins are placed adjacent to each pair of cells.
3. Magnesium is used throughout except for the two high end-pieces which are non-metallic.
4. Cooling for each cell is provided from two faces, one edge, and the bottom. Surfaces not cooled are the top and the second edge.

Table 4 SUMMARY OF BATTERY PACKAGING CONCEPTS

PACKAGING FEATURE		DESIGN CONCEPT																						
		1a	1b	2a	2b	3a	3b	3c	3d	4a	4b	4c	4d	4e	5a	5b	5c	5d	6a	6b	6c	7a	7b	7c
Layout	2 x 14 Cells	x	x	x	x	x		x	x	x	x	x												
	4 x 7 Cells												x	x	x	x	x	x	x	x	x			
	4-Cell Modules																					x	x	x
Manufacture	Formed Sheets						x	x	x				x								x	x	x	x
	Milling	x	x							x	x	x		x		x	x							
	Welding			x	x														x					
	Screw Joints					x	x		x	x					x			x	x	x				
	Bolt Joints						x	x	x		x	x	x	x		x	x				x	x	x	x
Heat Transfer ~ Surfaces of Cells	1 Edge	x																						
	2 Edges		x	x	x				x	x		x							x	x	x	x	x	x
	1 Face																						x	x
	2 Faces	x	x	x	x		x	x	x	x	x	x	x	x	x	x	x	x	x	x	x	x		
	Bottom	x	x	x	x		x	x	x	x	x	x	x	x	x	x	x	x	x	x	x	x	x	x
Stacking of Cells	Compact	x	x	x	x	x	x	x	x	x	x	x			x			x	x	x	x	x	x	x
	Gaps Between Rows												x	x		x	x							

Table 5 EVALUATION OF BATTERY PACKAGING CONCEPTS

KEY: Poor = 1
Fair = 2
Good = 3

CRITERIA	DESIGN CONCEPT																										
	1a	1b		2a	2b		3a	3b	3c	3d		4a	4b	4c	4d	4e		5a	5b	5c	5d		6a	6b	6c		7a	7b	7c
THERMAL:																													
. Temperature Rise	3	3		3	3		2	2	2	3		3	2	3	2	2		2	2	2	2		3	3	3		3	3	3
. Gradient in Cells	3	3		3	3		2	2	2	3		3	3	3	2	2		2	2	2	2		3	3	3		3	3	3
. Cell-to-Cell Symmetry	3	3		3	3		3	3	3	3		3	3	3	3	2		2	2	3	3		3	3	3		3	3	2
. Passive Temperature Control Potential	3	3		3	3		3	3	3	3		3	3	3	1	1		1	1	1	1		3	3	3		3	3	3
PARTS MANUFACTURE:																													
. Complexity	1	1		1	1		3	3	2	2		2	2	2	3	2		3	1	2	3		1	3	3		3	3	3
. Cost	1	1		1	1		3	3	2	2		2	2	2	3	2		3	2	2	3		1	3	3		3	3	3
. Schedule	1	1		1	1		3	3	2	3		2	2	2	3	2		3	2	2	3		1	3	3		3	3	3
ASSEMBLY:																													
. Tolerance Problems	2	2		2	2		3	3	2	3		2	2	2	2	2		2	2	2	2		2	2	2		2	2	2
. Trial Assembly Prior To Final Assembly	3	3		3	3		3	3	3	3		2	2	2	2	2		2	2	2	2		3	3	3		3	3	3
. Cell Replacement After Final Assy.	1	1		1	1		1	1	1	1		1	1	3	1	1		1	1	1	1		1	1	1		1	1	1
STRUCTURAL																													
. Strength and Rigidity	3	3		3	3		3	3	2	3		3	3	2	3	3		3	3	3	3		3	3	2		3	3	3
. Cell Bulging Restraint	2	3		3	2		2	2	2	3		3	3	2	2	2		2	3	3	2		3	3	3		3	3	3
. Thermal Surfaces Protect Cells	1	3		3	3		3	3	3	3		3	3	3	1	1		1	1	1	1		3	3	3		3	3	3
NASA COLD PLATE INTERFACE																													
. Bolt Accessibility	2	2		2	2		2	3	2	2		2	3	2	3	3		2	2	2	2		2	2	2		3	3	2
. Bolt-Nut Alighment	3	3		3	3		3	3	2	3		3	3	3	1	1		3	3	3	3		3	3	3		3	3	3
SIMILARITY TO FLIGHT DESIGN	3	3		3	1		2	2	1	3		1	1	2	1	1		2	2	2	1		3	3	1		1	1	1
GAS MANIFOLDING	3	3		3	3		3	3	3	1		3	3	3	3	3		3	3	3	3		3	3	3		1	1	1
ELECTRICAL WIRING	3	3		3	3		3	3	3	3		3	3	3	3	3		3	3	3	3		3	3	3		1	1	1
WEIGHT	3	3		3	3		3	3	3	3		3	3	3	3	3		3	3	3	3		3	3	3		3	3	3

RECOMMENDATION

MOCKUP OF BATTERY PACKAGE

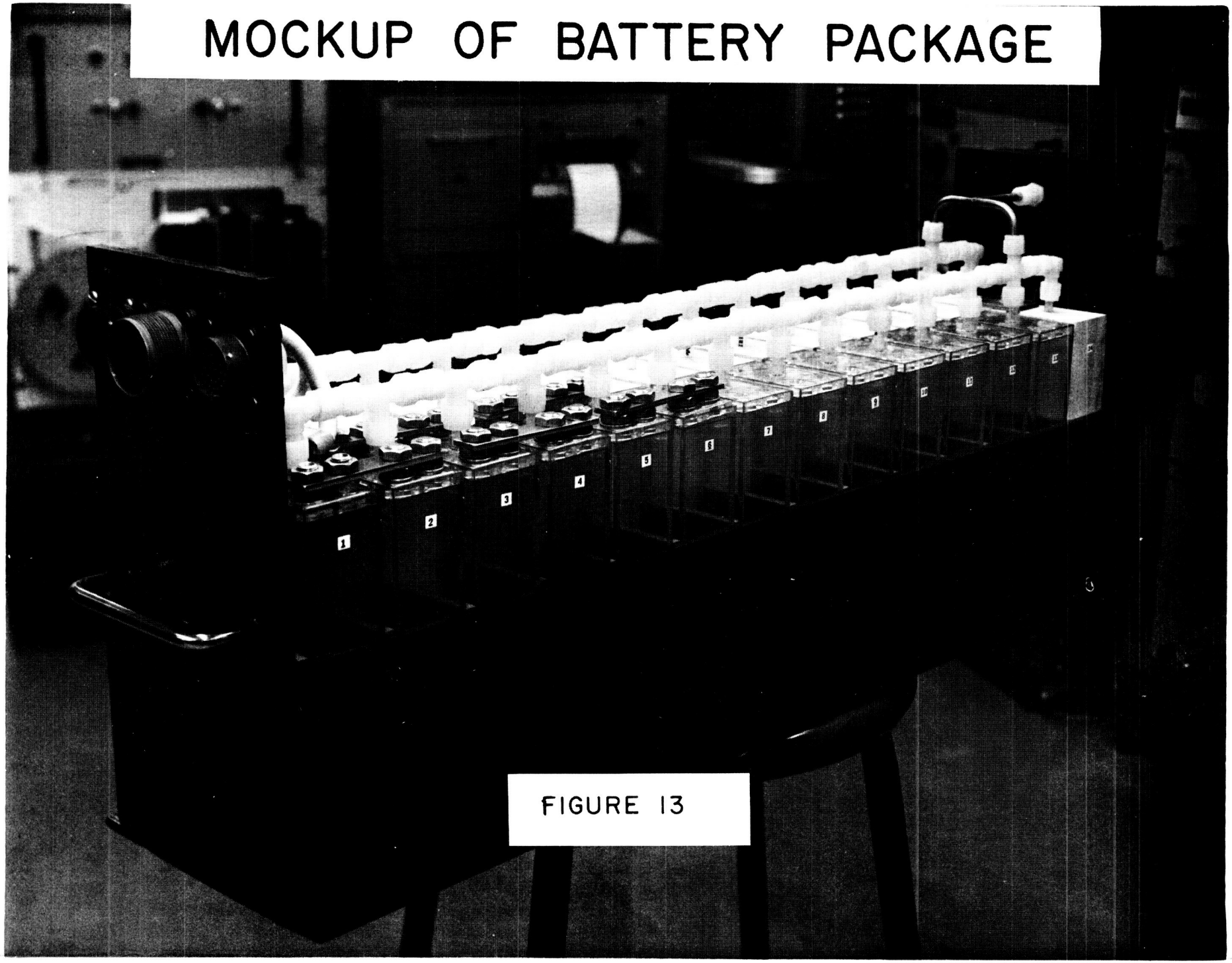

FIGURE 13

5. Two cell venting manifolds are mounted above the cells. The manifolds consist of polyethylene tubing with nylon Swagelok fittings.
6. Connectors for power and instrumentation are located at one end of the battery. Pressure instrumentation is housed at the other end.
7. Attachment to the NASA cold plate is made by bolting into threaded inserts in the bottom of the battery. NASA will be given a drill template to locate bolt holes in the cold plate.

Cell Selection and Matching

Cells received from the vendor will be tested to cull out defective cells. The cells will then be grouped into eight closely matched sets. Close quality control during manufacture is believed to be the most important step in assuring a close match, but tests will be conducted nevertheless in order to improve the match.

Unfortunately, there is no test yet available that will give an early prediction of future performance difficulties. A test to reveal internal shorts is the only one believed to have merit, and this will be used to help cull out suspicious cells. This test, which was tried out on silver cadmium cells, consists of these steps:

1. Fully discharge all cells.
2. Replace 0.5 percent of the cell capacity by charging.
3. Record open circuit voltage decay with time (bad cells decay fast).

Matching of cells will be done primarily on the basis of capacity. We have found, however, that though some cells of a group have the same capacity, they will often differ somewhat in other respects. Therefore, we believe that some weight should be given to factors other than capacity. In order to experiment with matching based on multiple criteria, tests

were conducted on three ampere-hour silver cadmium cells. Matching for selection of battery units was accomplished with the assitance of a computer program in which a weighting factor, based on judgment, was assigned to each of the following:

1. Charge ampere hours at constant current to a limiting voltage.
2. Capacity at constant current discharge to a limiting voltage.
3. Remaining capacity at discharge from limiting voltage to 0.1 volts.
4. Charge ampere hours at transition from lower plateau to upper plateau.
5. Upper plateau voltage (mid-range) during charge.
6. Lower plateau voltage (mid-range) during discharge.

6. THERMAL ANALYSIS

REQUIREMENTS

A contract requirement is a detailed thermal analysis which will predict accurately heat generation and temperatures over a wide range of operating modes. A computer program for performing the thermal analysis is to be delivered.

WORK COMPLETED

Heat Generation

The heat generation in 70-AH silver cadmium cells has been measured to obtain data for establishing a correlation method. The experimental procedure used was to encapsulate a cell in water-proofed foam, place it in a water bath closely-controlled in temperature, and cycle the cell until thermal and electrochemical repeatability is attained. Transient cell and water bath temperatures, cell current, and cell voltage were recorded. Using the foam as a calibrated thermal resistance, instantaneous heat generation rates were determined using the equation

$$q = \text{heat conducted} + \text{heat stored}$$

$$q = K(T - T_s) + MC_p \frac{dT}{d\theta}$$

where q = heat generation rate
K = insulation constant
T = cell temperature
T_s = sink temperature
M = cell weight
C_p = cell specific heat
θ = time

The insulation constant, K, is determined by an energy balance over a complete cycle of duration θ_t, using the temperature, voltage and current data; thus

$$K \int_0^{\theta_t} (T - T_s)\, d\theta = \int_0^{\theta_t} VI\, d\theta - W_{gas}$$

in which W_{gas} is a minor correction for energy devoted to irreversible gassing.

Typical experimental heat generation data obtained is shown in Figure 14. Heat generation rates during discharge are noted to be higher than during charge, which is typical. Also of interest is the slight negative heat flow during the first part of charge, which is due to the reversible entropy change that occurs at this time.

A correlation of heat generation with battery electrical parameters is desirable for making accurate thermal predictions over a wide range of operating conditions. To get this correlation, a procedure has been developed for expressing heat generation in terms that are related to battery chemistry. The expression derived for instantaneous heat generation is

$$q = I \left[V - \epsilon E_{\Delta H} - (1 - \epsilon) E_{\Delta H,\, O2} \right]$$

where:

q = heat generation rate in watts;

I = current in amperes (Positive for charge, negative for discharge)

ϵ = current efficiency (1.0 or less for charge, 1.0 for discharge)

V = cell terminal voltage

$E_{\Delta H}$ = enthalpy voltage corresponding to the heat of reaction, equal to $\frac{\Delta H}{ZF}$

where ΔH is the enthalpy change, Z is the number of electrons per molecule reacted, and F is a Faraday.

TYPICAL HEAT GENERATION TEST

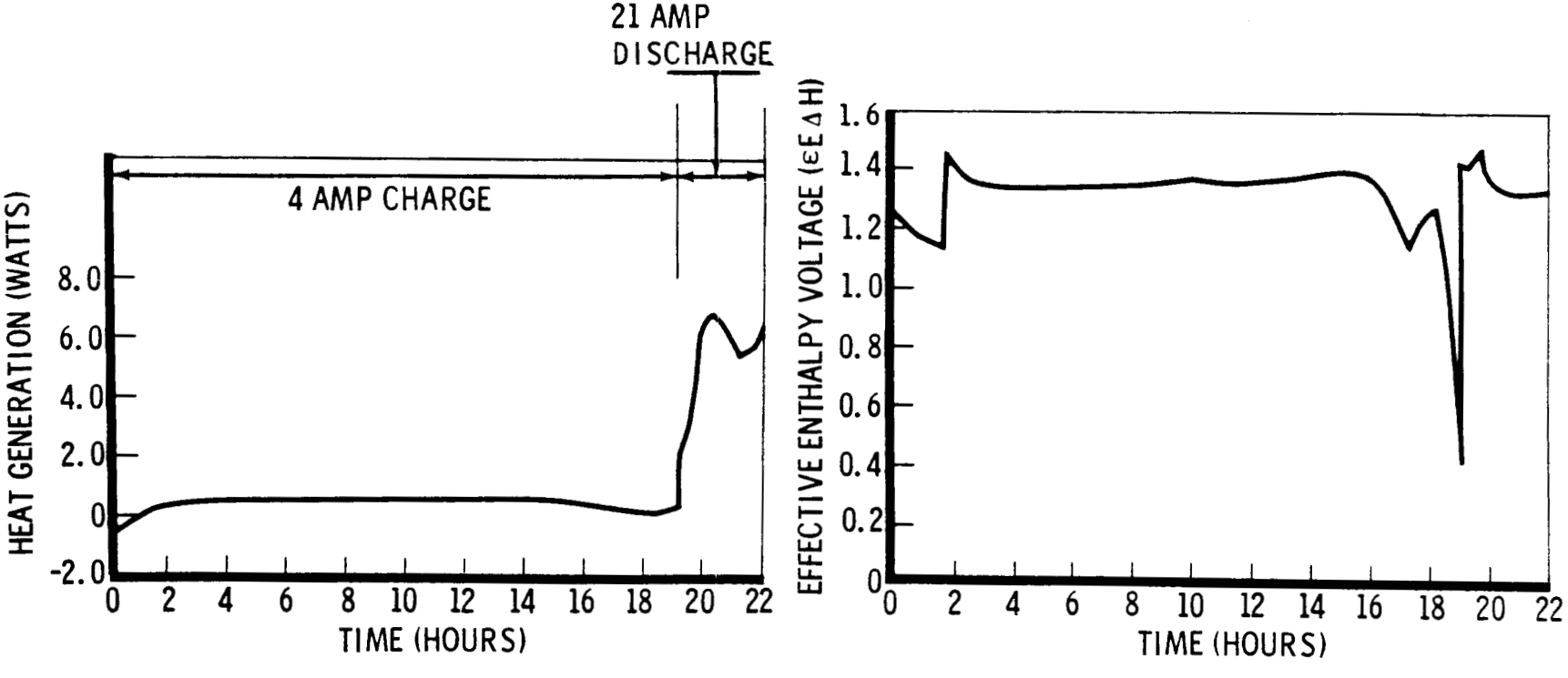

FIGURE 14

If there were only one chemical reaction, $E_{\Delta H}$ would be constant throughout charge and discharge. Since there are several simultaneous reactions occuring at different rates, $E_{\Delta H}$ is not quite constant.

The last group of terms in the correlation expression is important only if a substantial amount of gassing is permitted. Under proper charging, less than one or two percent of the energy change would be associated with this gassing effect.

The right half of Figure 14 shows the correlation of calculated heat generation with measured heat generation. In this example some of the correlation terms have been combined to result in an equation of the form

$$q = I \left[V - \epsilon E_{\Delta H} \right]$$

Temperature Prediction

The temperature of the battery will be predicted by means of an analytical network model of the real system, solved with a digital computer. The model consists of lumped-mass nodes, heat sources at the nodes, and radiation and solid conductors between nodes. The equation which is solved by the computer is

$$t_i^+ = t_i + \frac{\Delta \tau_i}{C_i} \left[\sum_j K_{ji} \ (t_j - t_i) + S \right]$$

where t_i^+ is the future temperature of a typical node i with heat transfer to j other nodes. The present temperature is t_i, thermal capacitance is C_i, heat sources are designated S_i, conductors are K_{ji}, and time is τ_i. Knowing the present temperatures, this equation is applied to each node to yield new temperatures for the complete network.

In order to obtain thermal conductance data, tests were performed on a 70 ampere-hour silver cadmium cell. The cell was placed in series with a material of known thermal conductivity, and the temperature gradients were

compared. Figure 15 shows the test arrangement. Plexiglas Type 2 was chosen as the comparison material because its thermal conductivity is in the proper range and is known accurately.

Test results show that the apparent thermal conductivity parallel to the plates is 0.42 BTU/Hr, ft^2, °F/ft; and perpendicular to the plates the conductivity is 0.27 BTU/Hr, ft^2, °F/ft. Results were found to be the same for both a charged cell and a discharged cell, within the experimental error. Also, the experimental results showed fair agreement with theoretical predictions, which gives confidence in the method being used.

Temperature prediction efforts have been applied to providing design criteria for battery packaging, as previously discussed. To do this, detailed analytical model of a single cell was made, and was used to obtain the data shown in Figures 11 and 12. A refinement of this thermal model will be used in the final temperature prediction program.

The computer program for temperature prediction is shown schematically in Figure 16. Heat generation is predicted in a subroutine. Mission and power system operation variables are supplied in the form of current and voltage versus time, and experimental values of enthalpy voltage are also inputed. This subroutine will be used in two analytical models. One is a microscopic model which will give fine resolution of temperature gradients within a cell, and will calculate data of a type that cannot easily be measured. The microscopic model will have more than 500 nodes. It will be useful in predicting effects of cell or packaging improvements, and in analyzing effects of non-uniform design or heat generation.

The second analytical model will be a macroscopic battery model. Its function is to determine temperature gradients that can occur over the entire package. The model will show the effects of cell imbalance, non-symmetrical packaging, and cold plate asymmetry. This model is not yet defined.

CELL THERMAL CONDUCTIVITY TEST ASSEMBLY

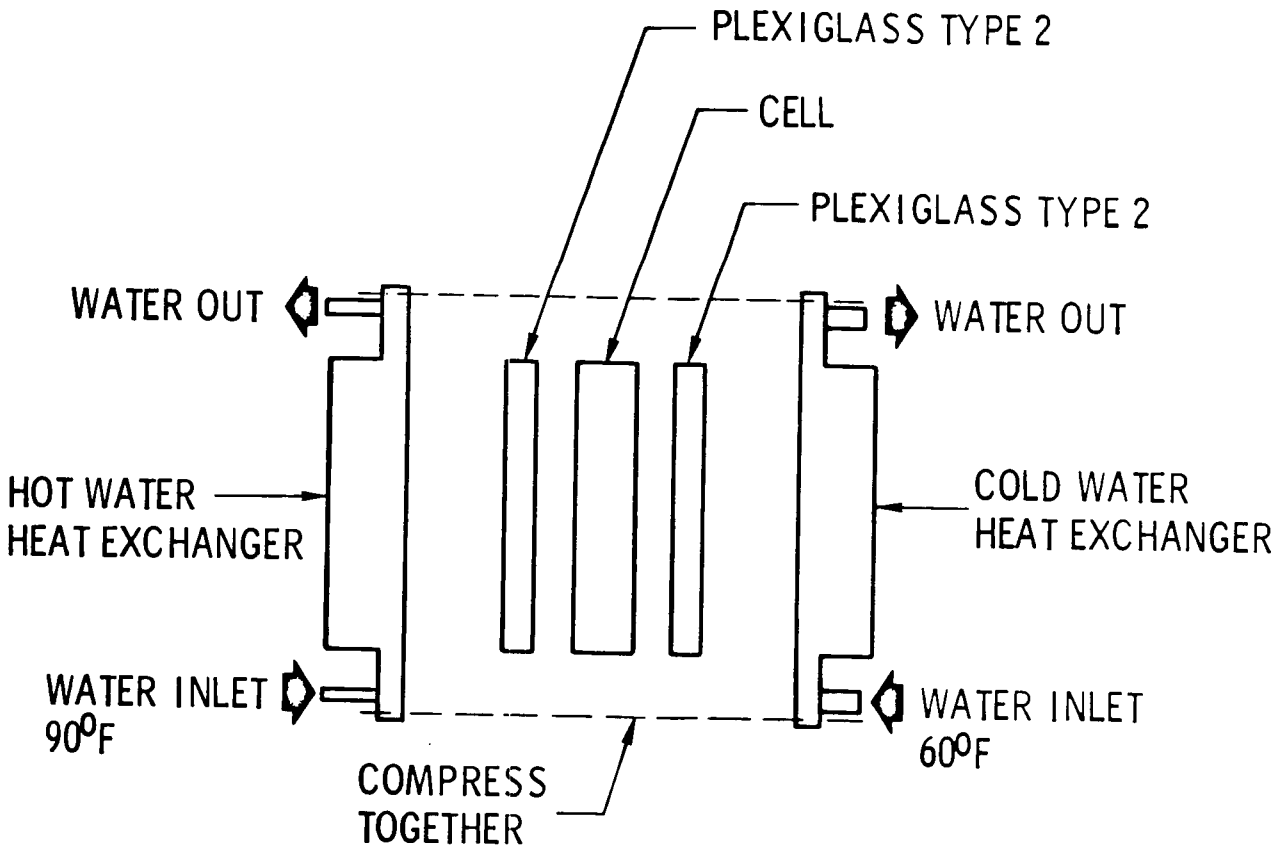

FIGURE 15

TEMPERATURE PREDICTION PROGRAMS

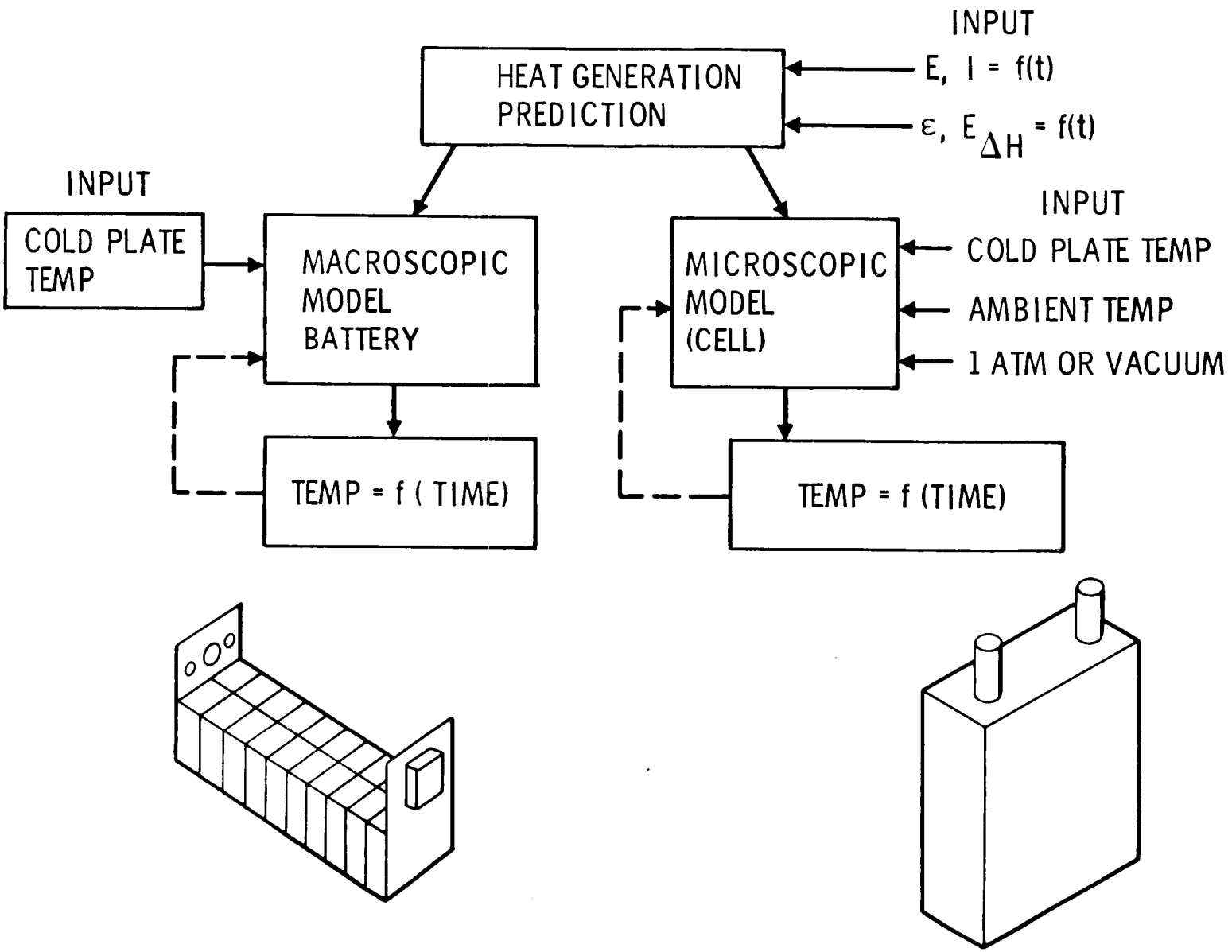

FIGURE 16

7. CALORIMETER DESIGN

REQUIREMENTS

A contract requirement is the design and fabrication of two calorimeters for detailed measurement of internal heat generation in the batteries. In addition, it is required that two batteries be specially instrumented for calorimeter tests.

WORK COMPLETED

The calorimeter concept planned is shown in Figure 17. The NASA-furnished coldplate normally used in tests is replaced by a heat exchanger designed for thermal measurements, and the battery-calorimeter assembly is insulated to minimize heat exchange with the environment. Heat input to the fluid is determined by measurement of fluid flow rates and inlet and outlet temperatures. Heat stored is measured by recording battery temperature change with time. The heat generated is then equal to the sum of heat flow to the fluid plus heat stored in the battery and calorimeter.

This approach to calorimetry was chosen for these reasons:

1. This method will determine heat generation rates effectively.
2. Temperature distribution in the battery during heat generation testing will be the same as during other tests. Therefore, battery chemistry should be the same.
3. Heat generation rates will be separated into realistic proportions between heat stored and heat rejected, which is a necessary breakdown to design the thermal control system.
4. The calorimeter can serve as a cold plate prior to and following heat generation testing. Therefore, heat generation tests can be conducted without disrupting life tests.

The critical measurement in the calorimeter is the temperature change of the cooling fluid from inlet to outlet. This problem has been studied, and either of two alternatives may be used effectively. One method is to

CALORIMETER CONCEPT

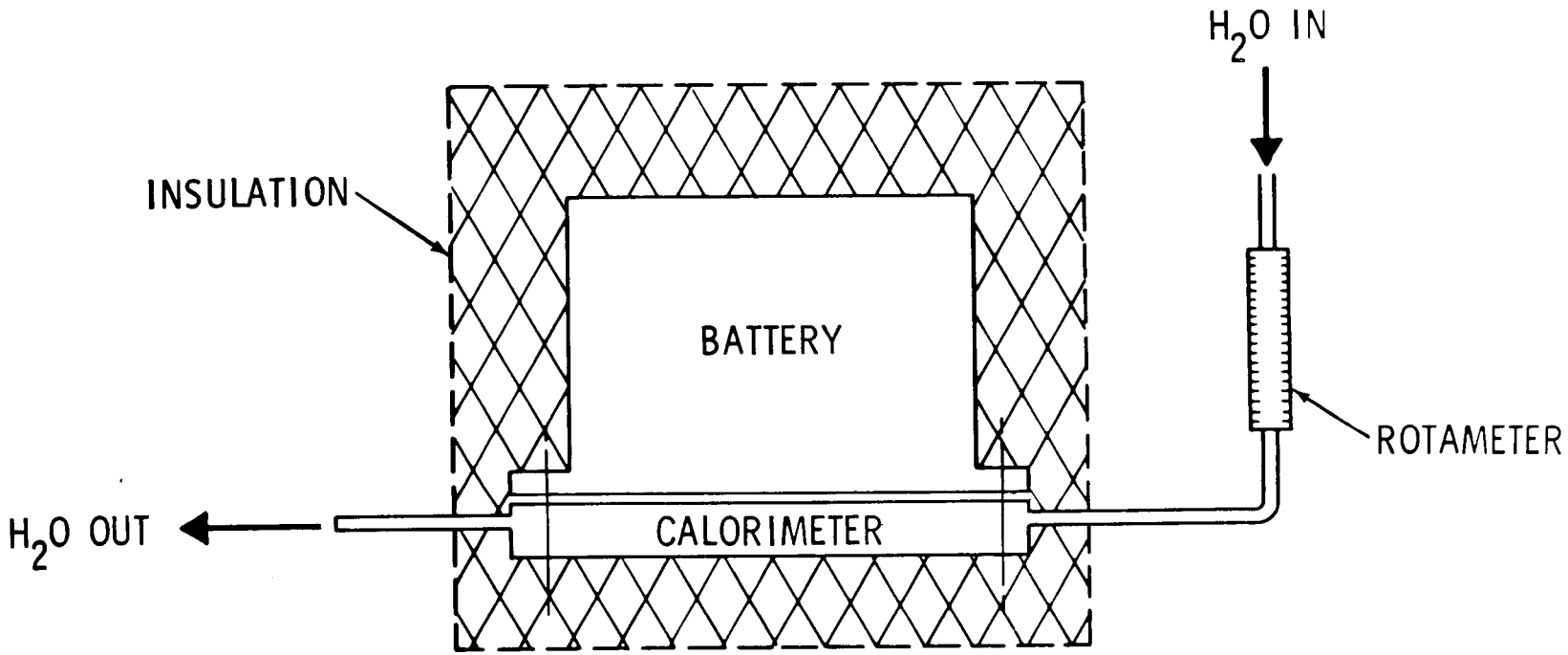

HEAT GENERATED = HEAT TO FLUID + HEAT STORED

MEASUREMENTS

1. BATTERY TEMP _____ THERMOCOUPLES
2. FLOW RATE _____ ROTAMETER
3. FLOW ΔT _____ THERMOPILE OR THERMISTERS

FIGURE 17

use a copper-constantan thermopile instrumented to sense temperature difference directly. The output voltage of the thermopiles will vary only 4 1/2 percent over the required 60°F to 90°F range with this approach. The other method is to use thermistors. However, the output of thermistors is not linear, so if we use thermistors we would use a linearization circuit of the type shown in Figure 18. The resistor values required are a function of the thermistor resistance and the beta factor of the thermistor. This circuit will provide an output voltage proportional to the temperature difference from inlet to outlet.

Experimental calorimetry work at Boeing has shown that it is very tedious to process the test data manually. We intend to furnish a computer program for processing this data, although the program is not specifically required by the contract. Inputs to the program will be temperature, flow rate and delta T versus time, insulation correction factors, and a fluid friction correction. The output of the program will be heat generation versus time, with separated into heat stored and heat to the fluid.

THERMISTORS TO MEASURE ΔT

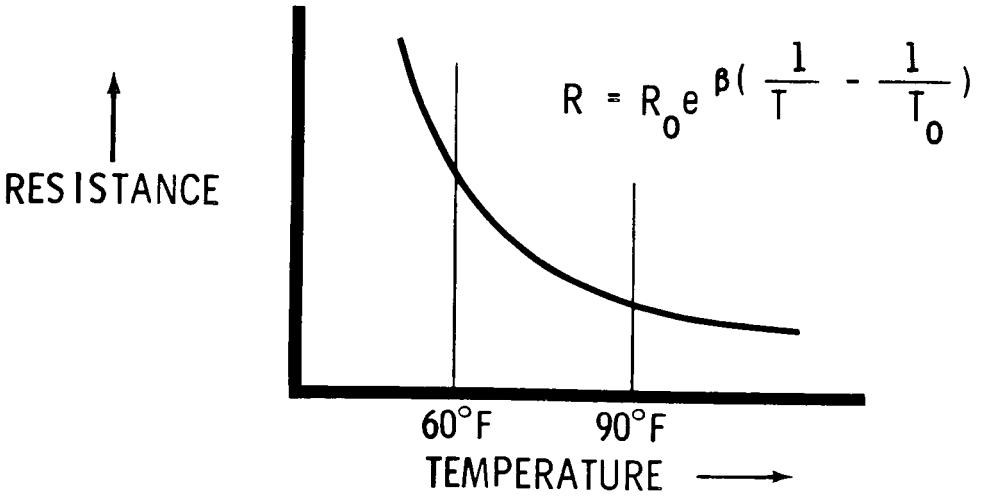

LINEARIZATION CIRCUIT:

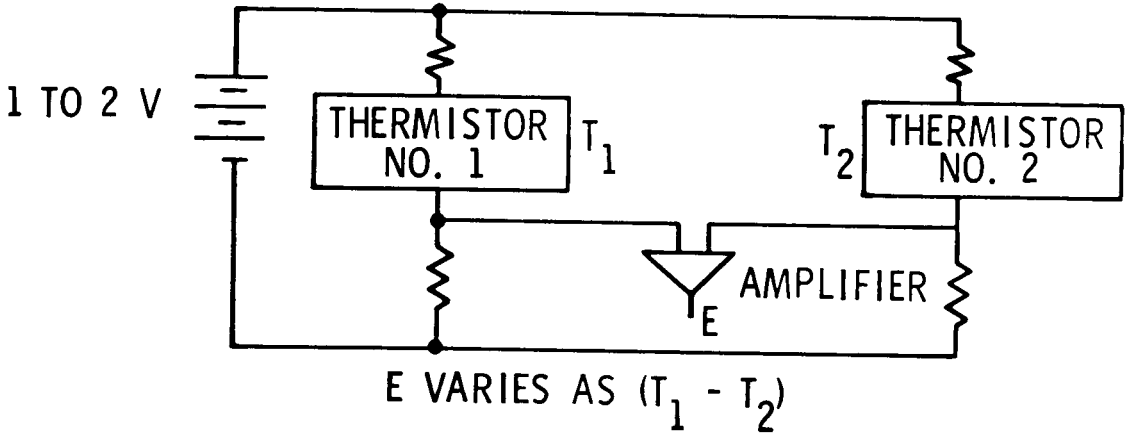

FIGURE 18

8. BATTERY CHARGE-DISCHARGE CONTROLLER

REQUIREMENTS

The Boeing Company is required to develop and provide four charge-discharge controllers for cycling the batteries. Two identical cabinets shall be provided, with two controllers in each cabinet. The controllers are identical, except that one has a manually-adjustable load, whereas the other has a programmable load. The manually-adjustable load must be variable up to at least 70 amperes. The programmable load must provide a minimum of 10 load levels on a single discharge cycle over a current range of 0.7 to 210 amperes, with individual "on time" adjustable from one second to two hours.

A variety of direct reading and analog readout instruments are required. Instruments requiring development are:

1. An ampere-hour meter with analog readout, reading up to 100 ampere-hours;
2. A watt-hour meter with analog readout and reading up to 2500 watt-hours.

WORK COMPLETED

Design of the charge-discharge controller has been completed. Commercially available components have been selected and ordered, and assembly of the cabinets has been started.

Battery Charge-Discharge Controller Description

A simplified functional diagram of the controller appears in Figure 19. Three shunts are used in each controller, one to measure charge current, another to measure discharge current, and the third to provide signals to the ampere-hour and watt-hour meters. Multiple shunts are used for current measurement because there is a large difference between the maximum charge current (20 amperes) and the maximum discharge current (210 amperes).

SIMPLIFIED CHARGE/DISCHARGE CONTROLLER

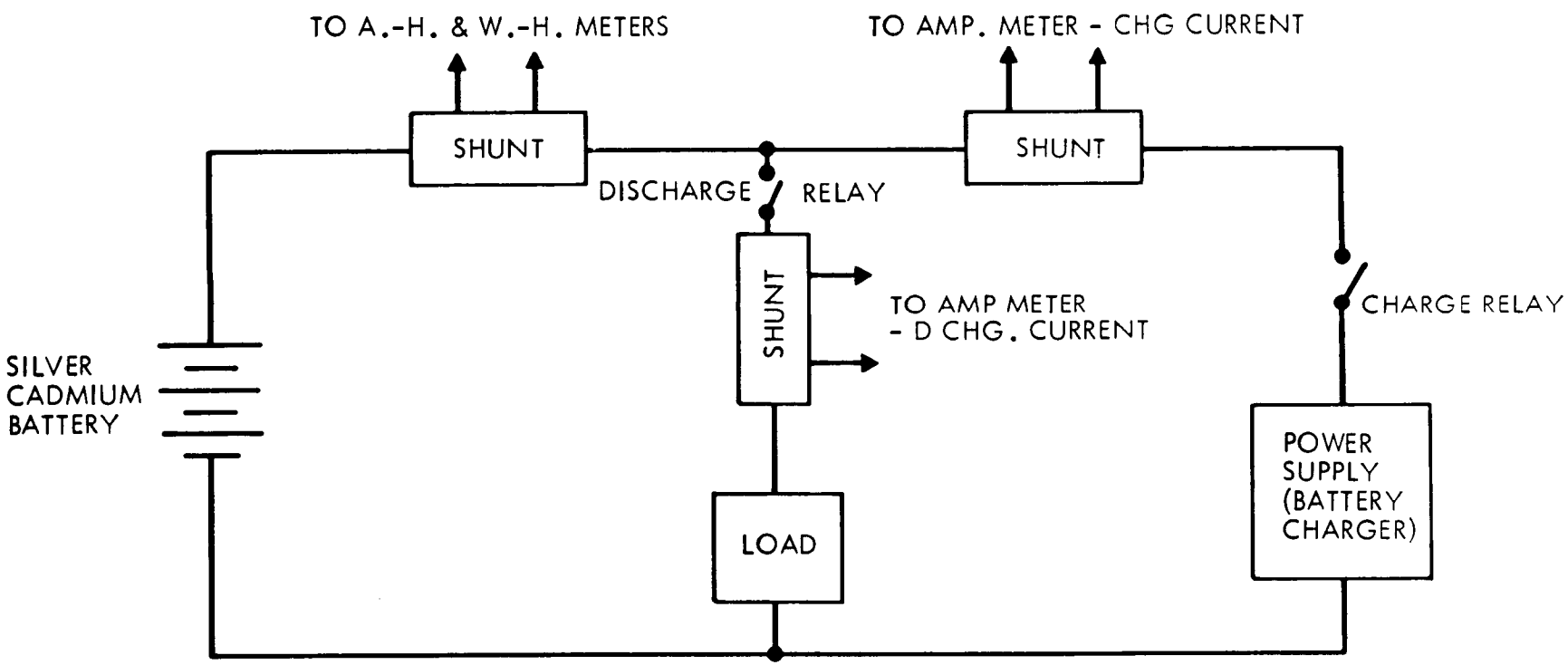

FIGURE 19

A Dual-Trol timer controls the charge-discharge cycle for the manually adjustable load, and a punched-tape programmer controls the charge-discharge cycle and load profile for the programmable load.

A block diagram of the controller appears in Figure 20, and the arrangement of components on the cabinet is shown in Figure 21. A schematic diagram of a cabinet containing two controllers is shown in Figure 22.

Manually Adjustable Load

The manually adjustable load is variable from 0.56 to 70 amperes, based on a 28 volt battery. A schematic of this load is shown in Figure 23. Closing switches 9 through 13 will provide a load current within 2.2 amperes of the desired value. Closing switch 8 connects in a rheostat having a range of 0.56 to 2.8 amperes for fine adjustment of current. Table 6 shows the combinations of switch positions that provide the required current or resistance values.

A recycling Dual-Trol timer controls the charge-discharge cycle for the battery connected to the manually adjustable load. This timer consists of two individual timing mechanisms which sequentially pulse a latch relay. One timing mechanism controls the charge duration, and the other controls the discharge duration. The timing mechanisms provide 0 to 3 hours discharge time, and 0 to 30 hours charge time.

Programmable Load

The programmable load provides any desired battery discharge current between 0.7 and 210 amperes in 0.7 ampere increments. A schematic of this load is shown in Figure 24. The load values are achieved by the closing and opening of relays. A separate channel in the punched tape programmer is assigned to each load relay. Table 7 shows the hole punches that provide the 305 possible load levels.

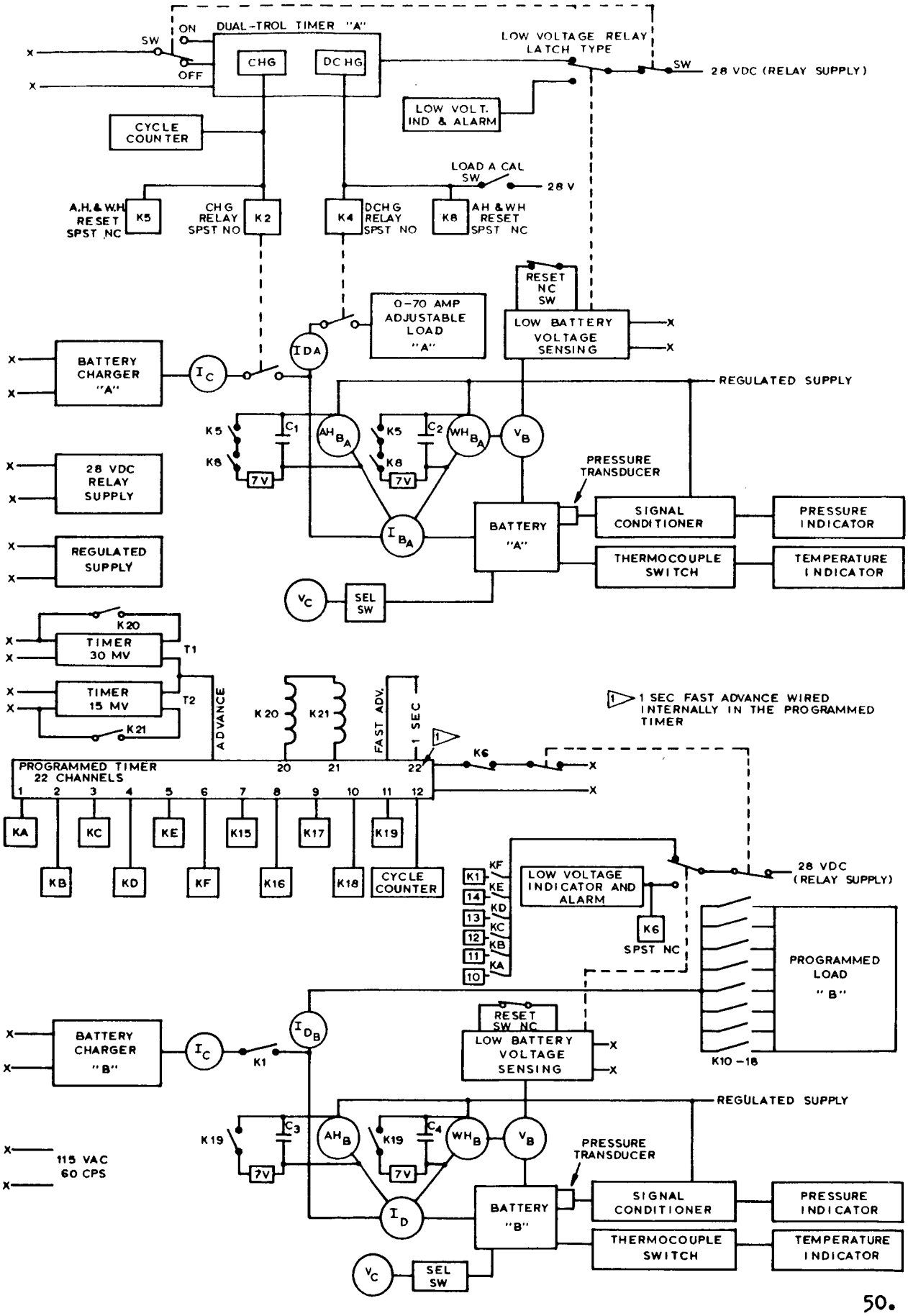

FIGURE 20 BATTERY CHARGE/DISCHARGE CONTROLLER BLOCK DIAGRAM

CHARGE/DISCHARGE CONTROLLER CABINET LAYOUT

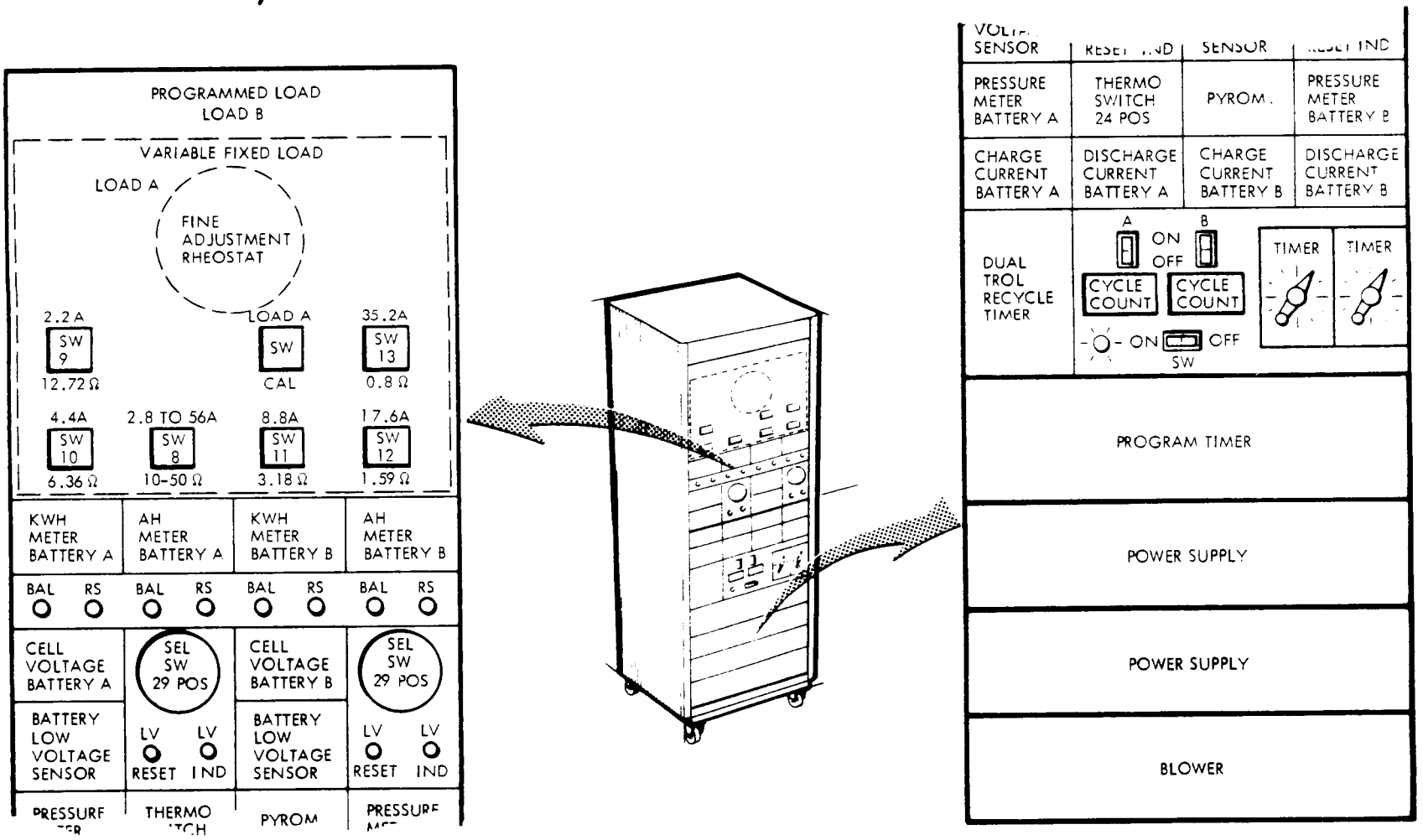

FIGURE 21

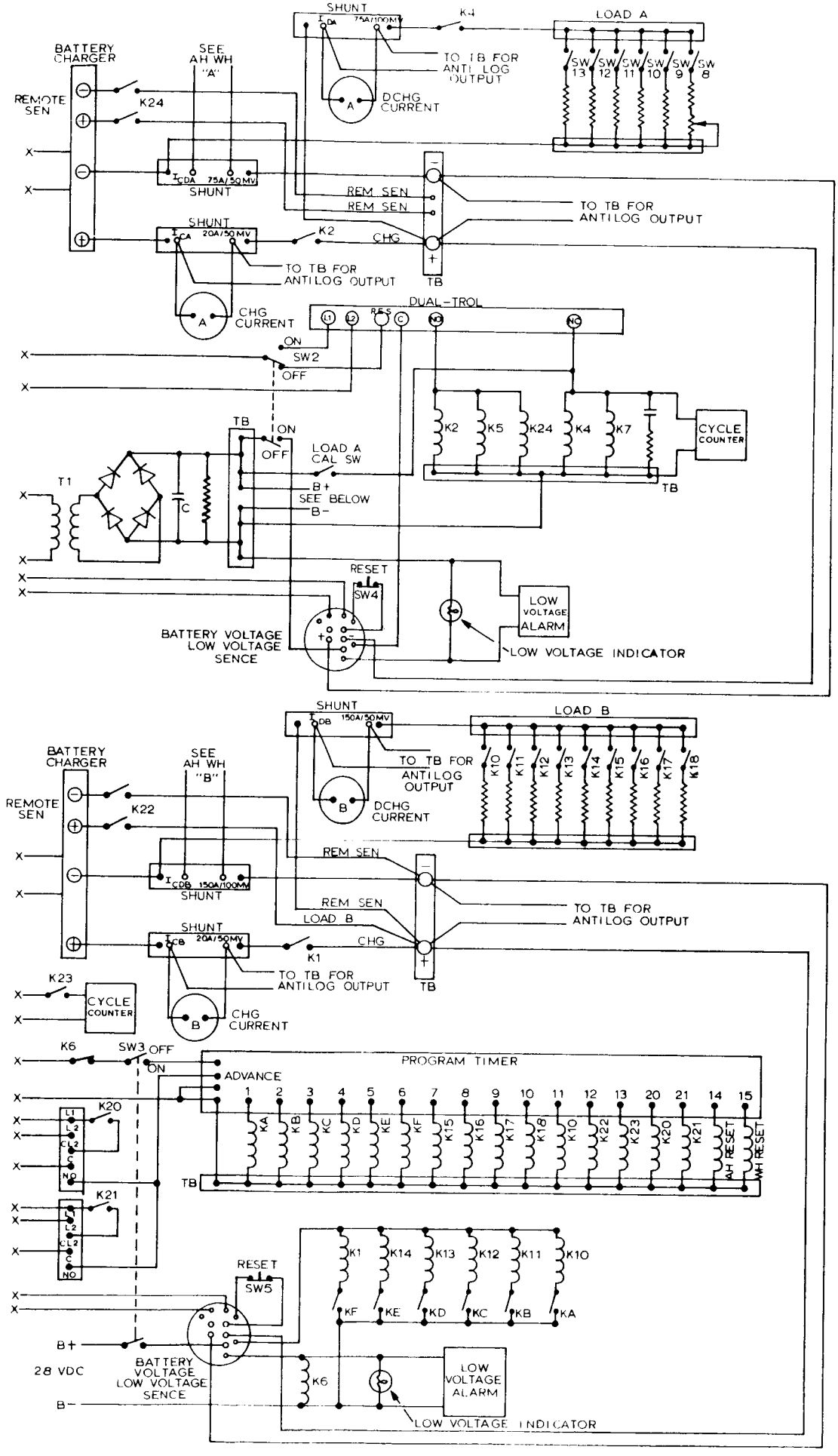

FIGURE 22
BATTERY CHARGE/DISCHARGE CONTROLLER SCHEMATIC

ADJUSTABLE FIXED LOAD

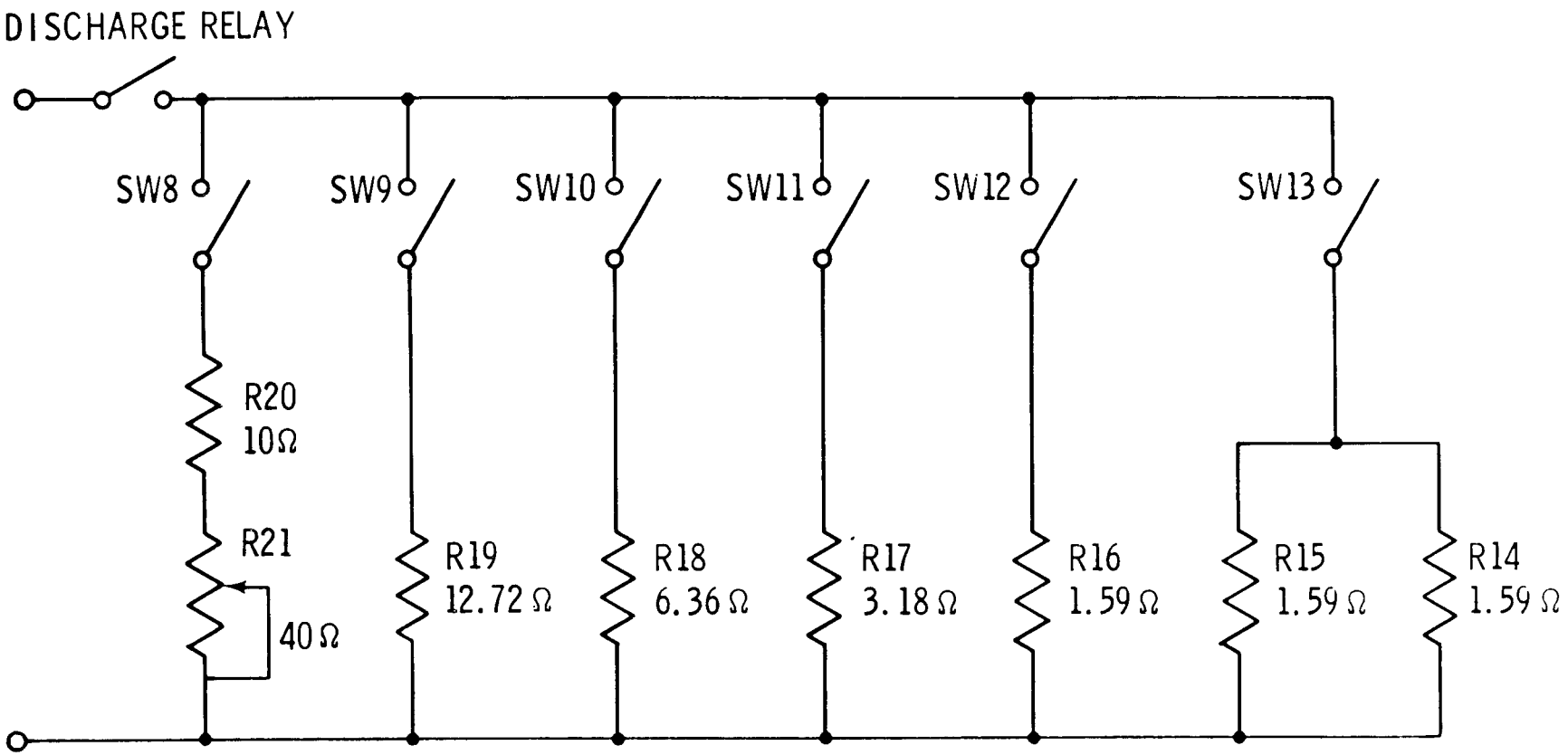

FIGURE 23

TABLE 6

SWITCH CLOSURES FOR FIXED LOAD SETTINGS

SWITCH	CURRENT RANGE - AMPERES*	RESISTANCE RANGE - OHMS
8	.56 - 2.8	50.000 - 10.000
8-9	2.71 - 5	10.332 - 5.600
8-10	4.96 - 7.2	5.645 - 3.889
8-9-10	7.16 - 9.4	3.911 - 2.979
8-11	9.36 - 11.6	2.991 - 2.414
8-9-11	11.56 - 13.8	2.422 - 2.029
8-10-11	13.76 - 16	2.035 - 1.750
8-9-10-11	15.96 - 18.2	1.754 - 1.538
8-12	18.16 - 20.4	1.542 - 1.373
8-9-12	20.36 - 22.6	1.375 - 1.239
8-10-12	22.56 - 24.8	1.241 - 1.129
8-9-10-12	24.76 - 27.0	1.131 - 1.037
8-11-12	26.96 - 29.2	1.039 - 0.959
8-9-11-12	29.16 - 31.4	0.960 - 0.892
8-10-11-12	31.36 - 33.6	0.893 - 0.833
8-9-10-11-12	33.56 - 35.8	0.834 - 0.782
8-13	35.76 - 38.0	0.783 - 0.737
8-9-13	37.96 - 40.2	0.738 - 0.697
8-10-13	40.16 - 42.4	0.697 - 0.660
8-9-10-13	42.36 - 44.6	0.661 - 0.628
8-11-13	44.56 - 46.8	0.628 - 0.598
8-9-11-13	46.76 - 49.0	0.599 - 0.571
8-10-11-13	48.96 - 51.2	0.572 - 0.547
8-9-10-11-13	51.16 - 53.4	0.547 - 0.524
8-12-13	53.36 - 55.6	0.523 - 0.504
8-9-12-13	55.56 - 57.8	0.504 - 0.484
8-10-12-13	57.76 - 60.0	0.485 - 0.467
8-9-10-12-13	59.96 - 62.2	0.467 - 0.450
8-11-12-13	62.16 - 64.4	0.450 - 0.435
8-9-11-12-13	64.36 - 66.6	0.435 - 0.420
8-10-11-12-13	66.56 - 68.8	0.421 - 0.407
8-9-10-11-12-13	68.76 - 71	0.407 - 0.394

* Based on 28 V dc input

PROGRAMMED LOAD

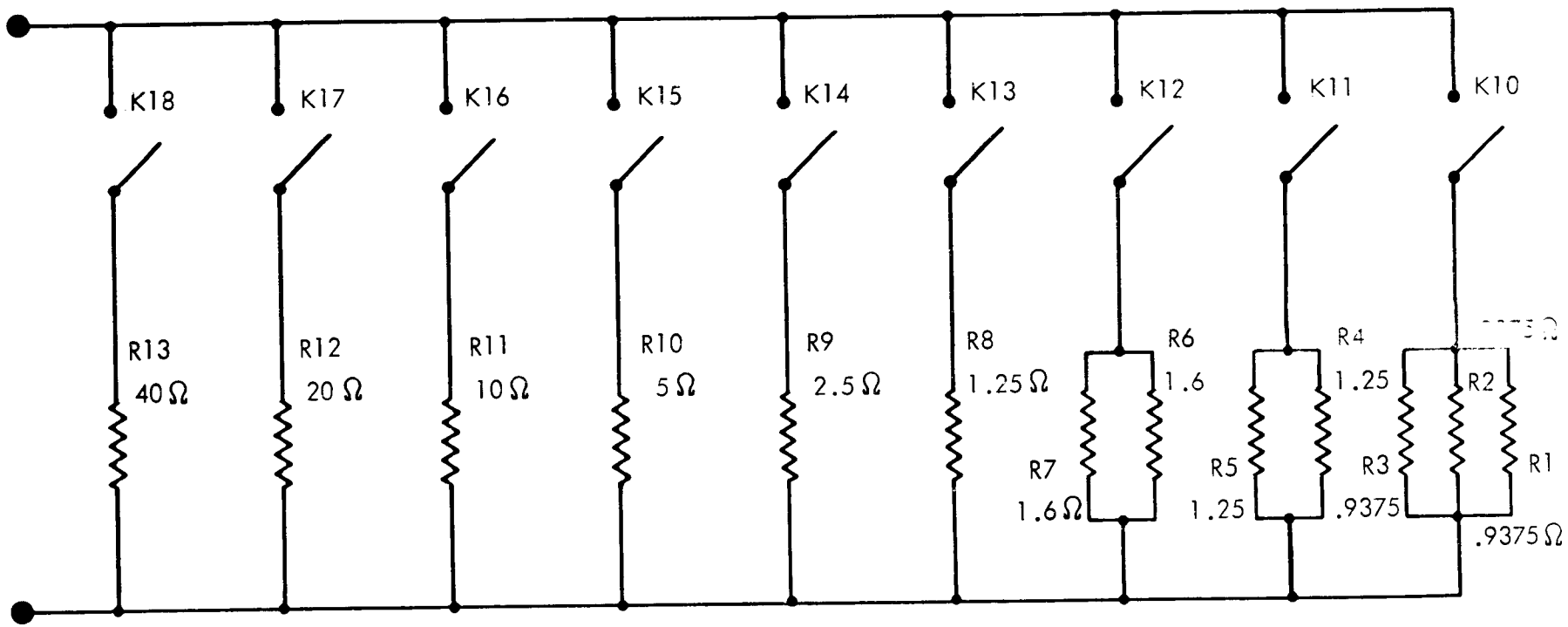

FIGURE 24

Table 7 PUNCHED TAPE COMBINATIONS FOR PROGRAMMABLE LOAD

I* (Amps)	R (Ohms)	Punch Channel 1 2 3 4 5 6 7 8 9
.7	40.0	x
1.4	20.0	x
2.1	13.333	x x
2.8	10.0	x
3.5	8.0	x x
4.2	6.666	x x
4.9	5.72	x x x
5.6	5.0	x
6.3	4.45	x x
7.0	4.0	x x
7.7	3.638	x x x
8.4	3.333	x x
9.1	3.078	x x x
9.8	2.857	x x x
10.5	2.666	x x x x
11.2	2.500	x
11.9	2.353	x x
12.6	2.221	x x
13.3	2.105	x x x
14.0	2.0	x x
14.7	1.905	x x x
15.4	1.84	x x x
16.1	1.74	x x x x
16.8	1.666	x
17.5	1.60	x x
18.2	1.538	x x
18.9	1.472	x x x
19.6	1.428	x x
20.3	1.38	x x x
21.0	1.332	x x x
21.7	1.29	x x x x
22.4	1.25	x
23.1	1.213	x x
23.8	1.175	x x
24.5	1.142	x x x
25.2	1.112	x x
25.9	1.081	x x x
26.6	1.051	x x x
27.3	1.027	x x x x
28.0	1.0	x
28.7	.986	x x
29.4	.953	x x
30.1	.930	x x x
30.8	.908	x x
31.5	.889	x x x
32.2	.870	x x x
32.9	.852	x x x x
33.6	.833	x x
34.3	.817	x x x
35.0	.80	x
35.7	.784	x x
36.4	.77	x x
37.1	.755	x x x
37.8	.742	x x
38.5	.727	x x x
39.2	.714	x x x
39.9	.703	x x x x
40.6	.69	x x
41.3	.678	x x
42.0	.666	x x
42.7	.656	x x x
43.4	.646	x x
44.1	.635	x x x
44.8	.625	x x
45.5	.6.6	x x
46.2	.607	x x
46.9	.598	x x x
47.6	.588	x x
48.3	.58	x x x
49.0	.572	x x x
49.7	.563	x x x x
50.4	.556	x x
51.1	.548	x x
51.8	.541	x x x
52.5	.533	x x x
53.2	.525	x x x x
53.9	.520	x x x x
54.6	.513	x x x x
55.3	.507	x x x x
56.0	.5	x x x x
56.7	.494	x x x x x
57.4	.492	x x
58.1	.483	x x x
58.8	.476	x x x
59.5	.471	x x x x
60.2	.465	x x x
60.9	.460	x x x x
61.6	.455	x x x
62.3	.449	x x x x x
63.0	.4447	x x x
63.7	.440	x x x x
64.4	.435	x x x x
65.1	.430	x x x x x
65.8	.426	x x x x
66.5	.4218	x x x x x
67.2	.417	x x x x
67.9	.4125	x x x x x
68.6	.408	x x x
69.3	.404	x x x x
70.0	.400	x x x x
70.7	.3965	x x x x x
71.4	.3922	x x x x x
72.1	.388	x x x x x
72.8	.3847	x x x x
73.5	.381	x x x x x
74.2	.3777	x x x x x
74.9	.374	x x x x x x
75.6	.3702	x x x x x
76.3	.367	x x x x x
77.0	.3642	x x x x x
77.7	.3608	x x x x x x
78.4	.3575	x x x
79.1	.354	x x x x
79.8	.3515	x x x
80.5	.348	x x x x
81.2	.345	x x x x
81.9	.342	x x x x
82.6	.339	x x x x
83.3	.336	x x x x
84.0	.333	x x x x
84.7	.331	x x x x x
85.4	.328	x x x x
86.1	.3252	x x x x x
86.8	.323	x x x x x
87.5	.320	x x x x x
88.2	.3175	x x x x
88.9	.3148	x x x x x
89.6	.3125	x x
90.3	.310	x x
91.0	.308	x x
91.7	.3053	x x x
92.4	.3035	x x x
93.1	.3009	x x x x
93.8	.299	x x x x
94.5	.2963	x x x x x
95.2	.294	x x
95.9	.292	x x x
96.6	.290	x x x x
97.3	.288	x x x x
98.0	.286	x x x x
98.7	.2837	x x x x
99.4	.2815	x x x x
100.1	.2797	x x x x x
100.8	.278	x x x
101.5	.276	x x x x
102.2	.274	x x x x
102.9	.272	x x x x
103.6	.2705	x x x x
104.3	.2683	x x x x x
105.0	.2665	x x x x x
105.7	.2652	x x x x x
106.4	.2635	x x x x
107.1	.2618	x x x x x
107.8	.260	x x x x x
108.5	.2582	x x x x x x
109.2	.256	x x x x x
109.9	.255	x x x x x
110.6	.2535	x x x x x
111.3	.2517	x x x x x x
112.0	.250	x x x
112.7	.2483	x x x x
113.4	.247	x x x x
114.1	.2468	x x x x
114.8	.246	x x x x x
115.5	.2432	x x x x x
116.2	.2415	x x x x x
116.9	.2397	x x x x x
117.6	.238	x x x x
118.3	.237	x x x x x
119.0	.2355	x x x x x
119.7	.2342	x x x x x
120.4	.2325	x x x x x
121.1	.2312	x x x x x
121.8	.230	x x x x x
122.5	.2287	x x x x x
123.2	.2275	x x x
123.9	.2261	x x x x
124.6	.2245	x x
125.3	.2233	x x x
126.0	.2223	x x x x
126.7	.2216	x x x x
127.4	.220	x x x
128.1	.2185	x x x x
128.8	.2175	x x x x
129.5	.2163	x x x x
130.2	.215	x x x x
130.9	.214	x x x x x
131.6	.213	x x x x x
132.3	.2117	x x x x x
133.0	.2109	x x x x x
133.7	.2097	x x x x x
134.4	.2085	x x x
135.1	.2076	x x x
135.8	.2062	x x x x
136.5	.2053	x x x x
137.2	.204	x x x x
137.9	.2032	x x x x
138.6	.202	x x x x
139.3	.2012	x x x x x
140.0	.200	x x x x
140.7	.1992	x x x x
141.4	.1982	x x x x
142.1	.197	x x x x x
142.8	.1961	x x x x
143.5	.1952	x x x x x
144.2	.194	x x x x x
144.9	.1932	x x x x x
145.6	.192	x x x x
146.3	.1917	x x x x
147.0	.1905	x x x x
147.7	.1898	x x x x x
148.4	.1888	x x x x x
149.1	.1878	x x x x x
149.8	.187	x x x x x
150.5	.1862	x x x x x
151.2	.1851	x x x x x
151.9	.1844	x x x x x
152.6	.1835	x x x x x
153.3	.1827	x x x x x
154.0	.1821	x x x x x
154.7	.1812	x x x x x x
155.4	.1804	x x x x x
156.1	.1793	x x x x x x
156.8	.1789	x x x x
157.5	.1778	x x x x
158.2	.177	x x x x
158.9	.1764	x x x x x
159.6	.1757	x x x x x
160.3	.1747	x x x x x
161.1	.174	x x x x x
161.7	.1734	x x x x x
162.4	.1725	x x x x x
163.1	.1717	x x x x x
163.8	.171	x x x x x
164.5	.1704	x x x x x
165.2	.1693	x x x x x
165.9	.1689	x x x x x x
166.6	.168	x x x x x
167.3	.1674	x x x x x x
168.0	.1665	x x x x
168.7	.1662	x x x x
169.4	.1652	x x x x
170.1	.1647	x x x x
170.8	.164	x x x x
171.5	.1632	x x x x x
172.2	.1626	x x x x x
172.9	.1621	x x x x x
173.6	.1615	x x x x x
174.3	.1607	x x x x x
175.0	.1600	x x x x x
175.7	.1594	x x x x x
176.4	.1587	x x x x x
177.1	.1583	x x x x x
177.8	.1574	x x x x x
178.5	.1568	x x x x x
179.2	.1562	x x x x x
179.9	.1558	x x x x x
180.6	.155	x x x x
181.3	.1547	x x x x x
182.0	.154	x x x x x
182.7	.1533	x x x x x
183.4	.1526	x x x x x
184.1	.1521	x x x x x
184.8	.1518	x x x x x
185.5	.1510	x x x x x
186.2	.1504	x x x x
186.9	.1499	x x x x x
187.6	.1495	x x x x x
188.3	.1487	x x x x x
189.0	.1482	x x x x x
189.7	.1478	x x x x x
190.4	.1470	x x x x x
191.1	.1466	x x x x x
191.8	.1460	x x x x
192.5	.1454	x x x x
193.2	.1450	x x x x
193.9	.1446	x x x x
194.6	.144	x x x x
195.3	.1434	x x x x
196.0	.143	x x x x
196.7	.1424	x x x x x
197.4	.1418	x x x x x
198.1	.1414	x x x x x
198.8	.1407	x x x x x
199.5	.1404	x x x x x
200.2	.1398	x x x x x
200.9	.1394	x x x x x
201.6	.1390	x x x x x
202.3	.1387	x x x x x
203.0	.1380	x x x x
203.7	.1377	x x x x
204.4	.1370	x x x x
205.1	.1367	x x x x
205.8	.1360	x x x x
206.5	.1357	x x x x
207.2	.1350	x x x x
207.9	.1348	x x x x
208.6	.1341	x x x x
209.3	.1339	x x x x
210.0	.1332	x x x x
210.7	.1330	x x x x
211.4	.1326	x x x x
212.1	.1320	x x x x
212.8	.1317	x x x x
213.5	.1312	x x x x

* Current Based on 28.0 Volts

The punched tape programmer (Figure 25) has 22 channels. It has brush contacts which complete circuits through holes in the tape (Figure 26). Channels in the punched tape are assigned to the load relays, time interval selection, control of charge and discharge events, and reset functions.

The punched tape is advanced in steps, one line at a time. The fastest advance is a fixed rate of one line per second. Thus, the load on the battery can be changed every second. Two adjustable timers provide stepping rates as low as one line per 30 minutes. Each of these three sources of stepping signals is controlled by a channel on the tape. Thus, the duration of a given load is established by the selection of the time delay to the next stepping operation.

All brush contacts on the programmer are "make before break". Thus, there will be no interruption in that portion of the load which is unchanged from one stepping period to the next.

The tape for the punched-tape controller, after being punched, can be spliced into a continuous loop so that the controller will repeat the charge and discharge cycle. Even the most complicated load cycles can be achieved with tape lengths of a few feet by the discrete use of the one-line-per-second and slower tape advances. Changes in the charge-discharge program can be made by splicing in new sections of tape, or by covering the appropriate punched holes with patching tape, and punching new holes as required.

Charge Control Method

The method of charge control is constant-current with limited voltage. This method is adequate for this application because the charge ampere-hours and discharge ampere-hours will not vary from cycle to cycle; therefore, the charge current can be set to obtain charge termination at any desired battery condition. Other charge control methods would be considered for actual space missions where the load is not fixed and repeatable. One of

PUNCHED TAPE PROGRAMMER

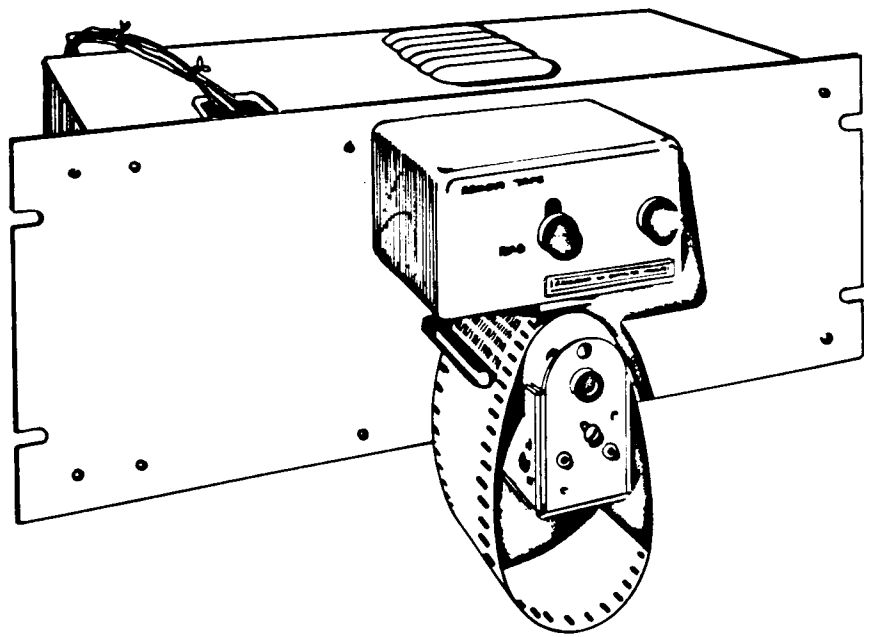

FUNCTION

- PROGRAMS CHARGE AND DISCHARGE EVENTS
- PROGRAMS LOADS FOR DISCHARGE
- PROVIDES TIME INTERVAL FOR EACH LOAD

FIGURE 25

PUNCHED TAPE PROGRAMMER

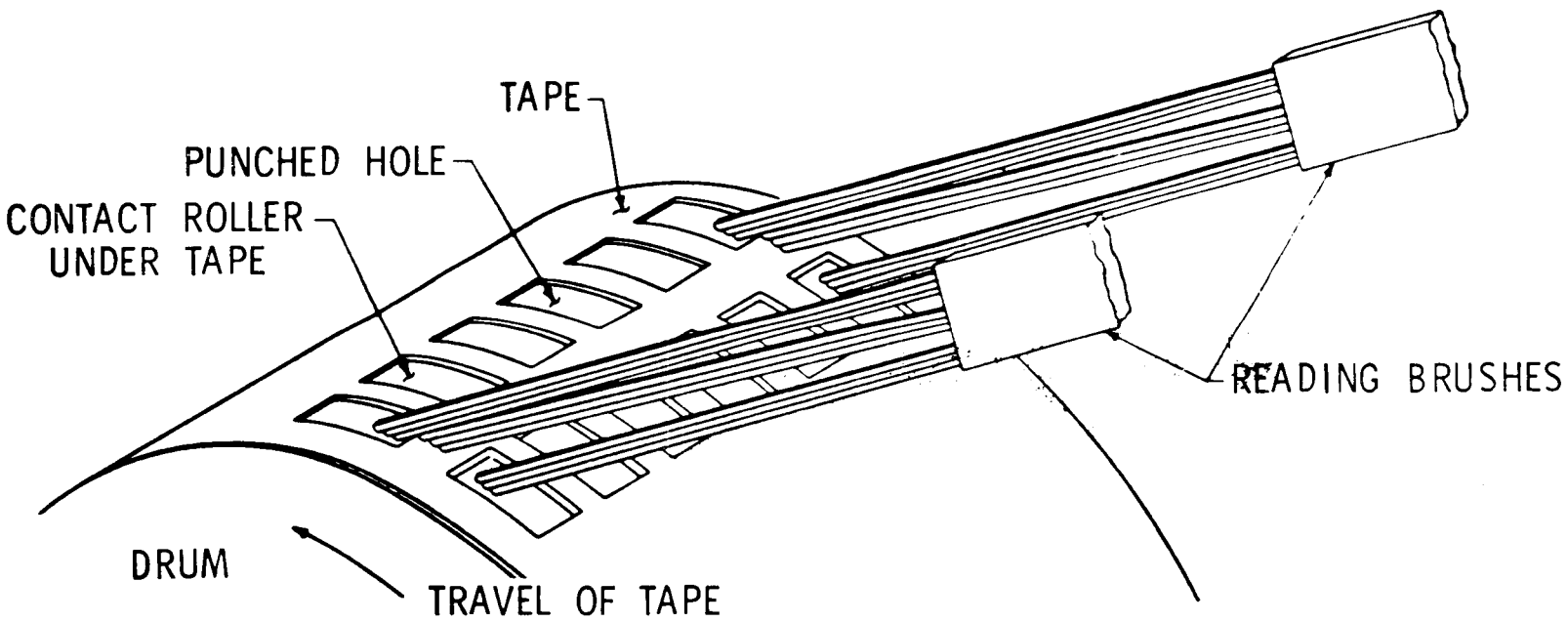

DESCRIPTION

- THE STEPPING DRIVE ADVANCES THE TAPE THROUGH THE READER LINE
- MOVEMENT OF THE TAPE OCCURS UPON RECEIPT OF PULSE
- PROVIDES A FAST ADVANCE WHICH TRANSPORTS THE TAPE AT ONE LINE PER SECOND

FIGURE 26

the most promising of these alternate charge-control methods is one in which current sensing terminates charge when the charge current has decayed to a predetermined level. The charge controller being furnished can be readily altered to simulate other charge control techniques.

Power Supply (Battery Charger)

Major factors in selecting the power supply were requirements for low ripple, close voltage regulation, and high stability. Low ripple is desired because of possible adverse effects on the battery. Close voltage regulation is necessary to prevent overcharge or undercharge. High stability prevents drift of the set point over a long period of time.

The power supply selected is made by Technipower, a Benrus subsidiary. Some of the operating characteristics of this unit are:

Regulation	± 0.01% + 2mv line; ± 0.03% + 6mv load
Ripple	500 microvolts RMS or 0.002%, whichever is greater
Stability	0.01% + 1mv for 8 hours after warmup.

This supply will automatically change the method of regulation from constant current to constant voltage. The constant voltage and constant current levels can be adjusted independently.

Current and Voltage Instrumentation

Charge current is measured across a 20-ampere, 50-mv shunt. Discharge current is measured with a 75-ampere, 50-mv shunt for the fixed load, and with a 150-ampere, 100-mv shunt for the programmed load. Analog output and one percent mirror-scale instruments are provided for monitoring current.

The cell-voltage and battery-voltage monitoring method is shown in Figure 27. Analog voltage output is provided for all the cells, and one percent mirror-scale instruments are provided for visual monitoring of cell voltage with a manual selector switch.

Battery voltage is monitored continuously with a separate voltmeter. This instrument has a low-voltage cutoff to terminate discharge when the battery voltage drops below a present level. The low-voltage cutoff portion of the

CELL VOLTAGE & BATTERY VOLTAGE MONITORING

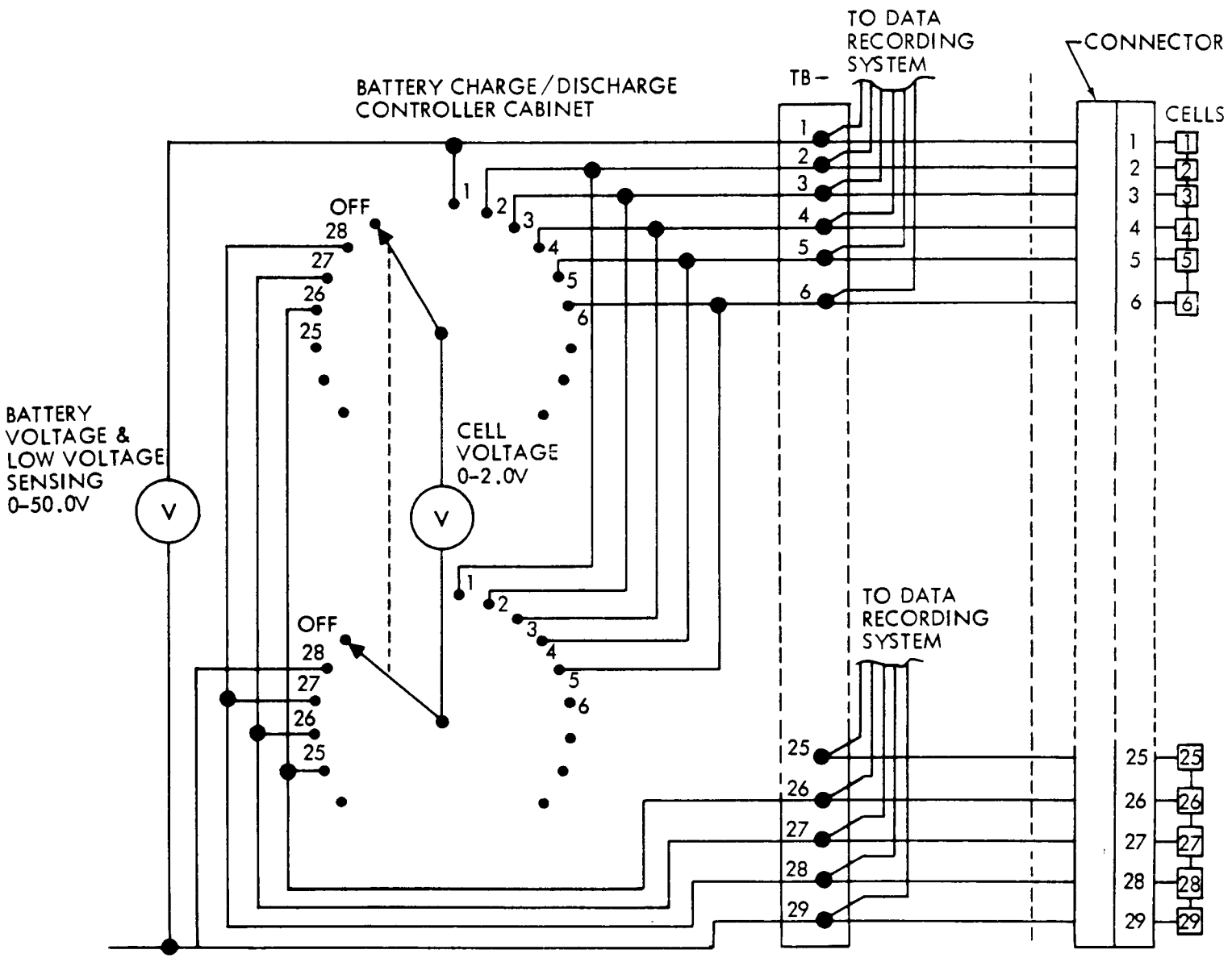

FIGURE 27

meter is a contactless meter-relay with a light source, a photoconducting cell, a mechanism to cut off the light at the set point, a bridge which turns off a silicon controlled rectifier (SCR) and a load relay actuated by the SCR.

Temperature and Pressure Instrumentation

Battery temperatures are sensed with copper-constantan thermocouples. The thermocouple outputs are monitored with a pyrometer using a manual selector switch (Figure 28). A terminal strip is also provided for the NASA-MSC data recording system.

Battery gas pressure is sensed by a strain-gage pressure transducer which requires a 7-volt dc power supply. The pressure is read on a millivolt meter, appropriately calibrated for a 0 to 25 psia scale.

Ampere-Hour and Watt-Hour Meters

Figures 29 and 30 show schematics of the ampere-hour and watt-hour meters. The ampere-hour meter uses an operational amplifier which integrates a voltage that is proportional to current. This voltage is developed across a shunt. The theoretical output of the amplifier is

$$E_{out} = \frac{1}{RC} E_{in} t$$

where R is resistance in ohms, C is capacitance in farads, and t is time in seconds. In order to minimize error, the capacitor must have a high insulation resistance, and the amplifier must have low offset current and voltage. The balance control reduces the error caused by offset current and voltage.

The watt-hour meter uses a Hall multiplier to obtain a signal that is proportional to the product of voltage and current. This signal is then integrated with an operational amplifier to obtain watt-hours.

THERMOCOUPLE MONITORING

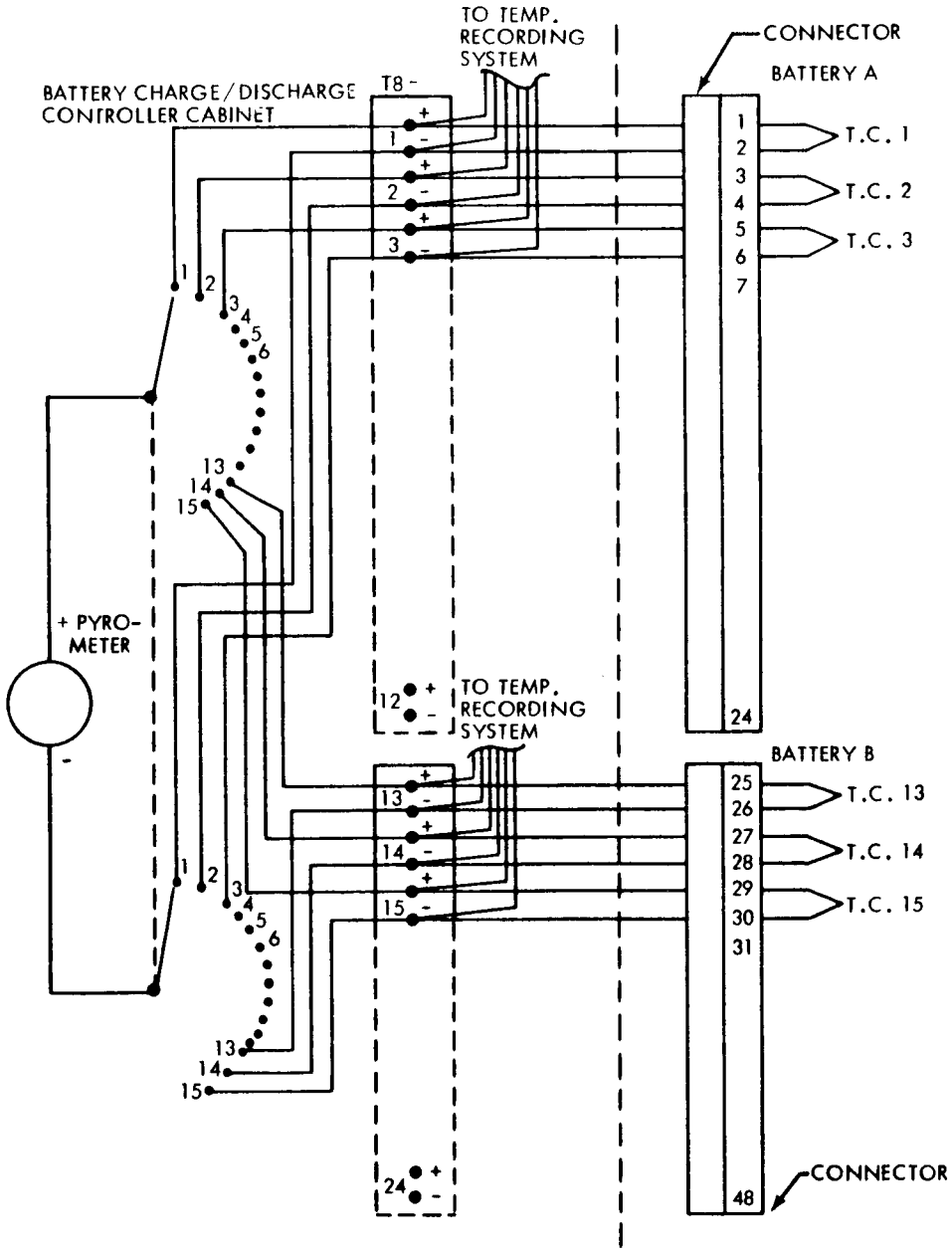

FIGURE 28

AMPERE-HOUR METER SCHEMATIC

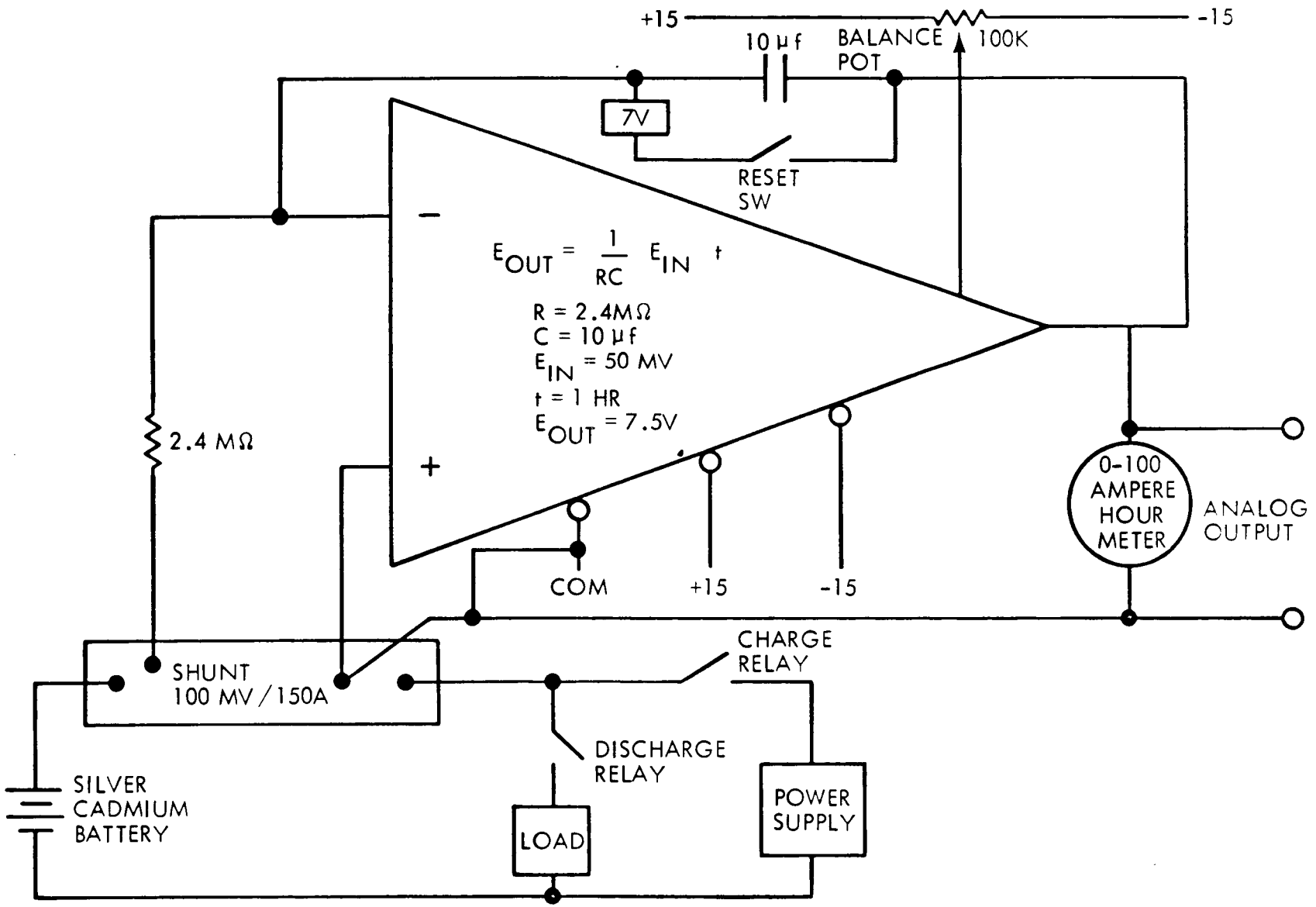

FIGURE 29

WATT-HOUR METER SCHEMATIC

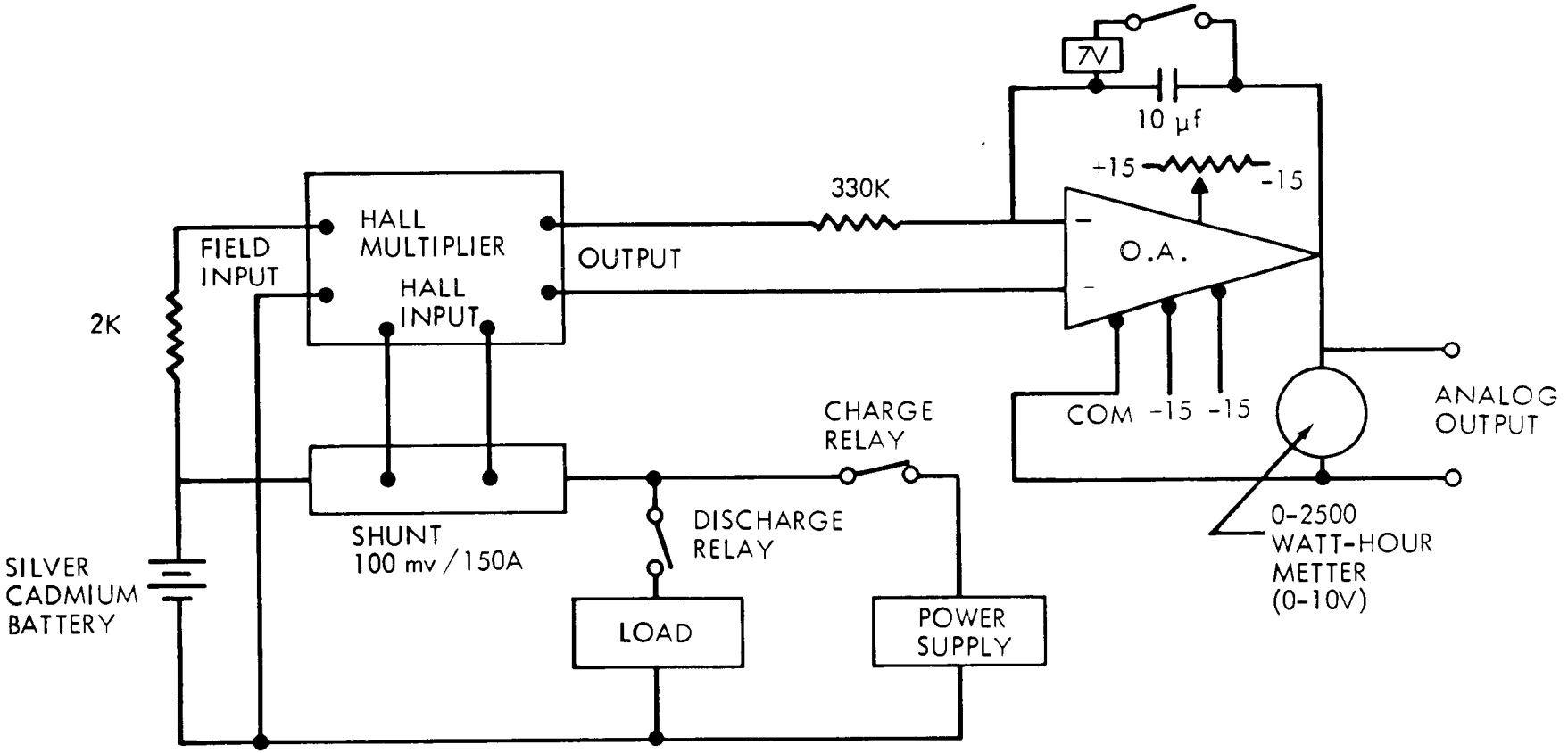

FIGURE 30